repeating unit in which three types of cyclobutane structures are incorporated in a sequence of $[\alpha\beta\epsilon\beta\alpha\beta^{-1}\epsilon\beta^{-1}]$, where β and β^{-1} are opposite in configuration to each other (see Figure 4). Considering the stereochemistry of cyclobutane, every two neighboring β-type cyclobutanes are opposite in configuration ("double syndiotactic"). From the viewpoint of synthetic polymer chemistry, although the formation of stereospecific polymers (isotactic and syndiotactic) is very popular, especially by using a Ziegler-type catalyst, the present polymer is the first example of the polymer having a double syndiotactic structure. In contrast, since the main product is only tetramer **4b** in the photoreaction of crystal **2b**, the ethyl ester side olefins doubtlessly still stay beyond the reactive distance, even after the pyridyl side olefins in **2b** have reacted. However, since the octamer was obtained without any other appreciable byproducts at room temperature, the structure of the octamer is expected to have a repeating unit in which two types of cyclobutane structures are arranged in a sequence of $[\beta\alpha\beta^{-1}\alpha]$ ("syndiotactic"), as shown in Figure 4.

Conclusions

The topochemical behavior of alkyl α-cyano-4-[2-(2-pyridyl)ethenyl]cinnamates (**1a** and **1b**) and their dimers (**2a** and **2b**) was investigated on the basis of crystallographic, mechanistic, and product analyses.

In the reaction of crystal **1a**, the product of the topochemical photoreaction was controlled not only by the wavelength of the irradiating light, but also by the irradiation temperature. The monocyclic dimer **2a** was a main product when **1a** was irradiated under various conventional irradiation conditions. On the other hand, at an extremely low temperature (−40 °C), the thermal motion of the monocyclic dimer **2a** was restricted; upon further irradiation, a highly strained tricyclic [2.2]paracyclophane (**3a**) was obtained as a major product. In the photoreaction of **1b**, the monocyclic dimer **2b** was obtained in very high yield over a wide range of irradiation temperatures (−40 to ~+90 °C). A phase change of amorphous **2b** into the crystalline state occurred upon annealing at 135 °C, or even during the photoreaction when sufficient thermal energy was supplied, and the tetramer **4b** was obtained by prolonged photoirradiation.

Although the photoreactions of **1** into **2**, and of **2** into **4** or polymer were reasonably interpreted by crystallographic analyses of **1** and **2**, the structure of the tetramer and the polymer were unpredictable from the crystal structures of the corresponding monomers. On the basis of the similarity between the crystal structures of **1b** and **2b**, it was concluded that the photoreaction of **1b** into **2b** and tetramer **4b** is topochemically controlled and is accompanied by a topochemical induction that causes the formation of an alternating arrangement of both enantiomers and a zigzag-linear structure. The formation of an alternating sequence of both enantiomers is the first demonstration of such a process through an organic reaction of prochiral molecules in an achiral environment.

Finally, very unique structures of the polymer and the oligomer, in which the cyclobutane structures are arranged in a sequence of $[\alpha\beta\epsilon\beta\alpha\beta^{-1}\epsilon\beta^{-1}]$ and $[\beta\alpha\beta^{-1}\alpha]$, respectively, were formed in the photoreaction of the dimer crystals **2a** and **2b** under crystal lattice control.

Acknowledgment. We thank Dr. S. Sato (Sankyo Co., Tokyo, Japan) for making available to us the crystallographic data of **1a**, **1b**, **2a**, and **2b**.

Registry No. 1a, 106366-65-8; **1b**, 124067-51-2; **2a**, 135413-74-0; **2a** (polymer), 135310-68-8; **2b**, 135413-75-1; **3a**, 135310-66-6; **4a**, 135413-76-2; **4b**, 135413-77-3; **5**, 135310-65-5; methyl cyanoacetate, 105-34-0; ethyl cyanoacetate, 105-56-6.

Supplementary Material Available: Molecular structures and tables of atomic coordinates, thermal parameters, bond lengths, and bond angles for **1a**, **1b**, **2a**, and **2b** (13 pages). Ordering information is given on any current masthead page.

Phytochrome Models. 11.† Photophysics and Photochemistry of Phycocyanobilin Dimethyl Ester‡

Silvia E. Braslavsky,* Dagmar Schneider, Klaus Heihoff, Santiago Nonell, Pedro F. Aramendia, and Kurt Schaffner

Contribution from the Max-Planck-Institut für Strahlenchemie, D-4330 Mülheim a. d. Ruhr, F.R.G. *Received April 10, 1991. Revised Manuscript Received May 20, 1991*

Abstract: Phycocyanobilin dimethyl ester (**3**) undergoes a self-sensitized oxidation by a singlet oxygen $[O_2(^1\Delta_g)]$ mechanism with a quantum yield of 10^{-5}–10^{-6}, depending on the solvent, excitation wavelength, and concentration. The main photooxidation products are a tripyrrolic aldehyde (**7**) and three stereoisomeric peroxides (**8**–**10**) formed from two units of **3**. Near-IR emission of $O_2(^1\Delta_g)$—formed upon sensitization by **3** under both steady-state irradiation and pulsed excitation—constitutes the first direct evidence for the intersystem crossing of a bilatriene. The low photooxidation yield results from a low intersystem crossing yield from **3**, $\Phi_{isc} < 10^{-4}$, estimated by the energy-transfer method in flash photolysis. A total rate constant of $k_q = (3.4 \pm 0.3) \times 10^8$ M^{-1} s^{-1} was determined for the quenching of $O_2(^1\Delta_g)$ by **3**. Possible relations between these findings and the photophobic movement of *Anabaena variabilis* are discussed. In analogy to biliverdin dimethyl ester, two types of conformations (a helical form and a family of stretched forms) for **3** [and for its 3,3′-dihydro-3′-thioethoxy derivatives (3′*S**)-**5**] were detected in methanol at room temperature by stationary fluorescence and excitation spectra. The wavelength dependence of the self-sensitized photooxidation of **3** is due to the selective reaction of the helical conformer, while a selective photoisomerization of the stretched forms of **3** and **5** was observed by time-resolved laser-induced optoacoustic spectroscopy. For **3** the latter process takes place with a quantum yield > 0.5, and the resulting isomer (probably a C-10 stereoisomer of the parent compound) reverts to the ground state with a lifetime of around 200 ns.

Introduction

Phytochromobilin (**1**) and phycocyanobilin (**2**), the bilatriene chromophores of the plant photoreceptor phytochrome and the algal pigment phycocyanin, respectively, have very similar structures (Scheme I). They differ only in the substitution of ring D: **1** possesses a vinyl group and **2** an ethyl group instead.[1] Since **2** is much more readily accessible from algae than **1** is from plants, this study was directed toward the photophysical and

† For Phytochrome Models. Part 10, see ref 6.

‡ This work is taken in parts from the Ph.D. Theses of D.S., Ruhr-Universität Bochum/MPI für Strahlenchemie, 1988, and of S.N., Institut Quimic de Sarriá/MPI für Strahlenchemie, 1988. It has been presented at the XIIth IUPAC Symposium on Photochemistry, Bologna, 1988.

(1) Scheer, H. *Angew. Chem., Int. Ed. Engl.* **1981**, *20*, 241–261.

0002-7863/91/1513-7322$02.50/0

Scheme I[a]

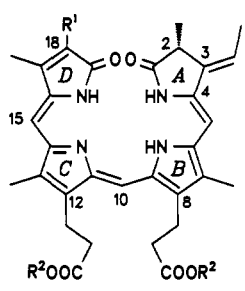

1 $R^1 = CH{=}CH_2$, $R^2 = H$
2 $R^1 = CH_2CH_3$, $R^2 = H$
3 $R^1 = CH_2CH_3$, $R^2 = CH_3$

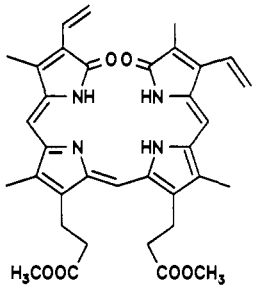

4

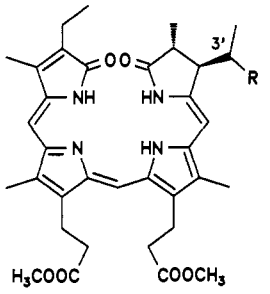

5 $R = SCH_2CH_3$
6 $R = OCH_3$

[a] Helically coiled all-*Z*,all-syn conformations of phytochromobilin (**1**), phycocyanobilin (**2**) and its dimethyl ester (**3**), biliverdin dimethyl ester (**4**), and the 3′-epimeric 3,3′-dihydro-3′-thioethoxy- and -3′-methoxyphycocyanobilin dimethyl esters **5** and **6**.

photochemical properties of phycocyanobilin dimethyl ester (**3**) as a phytochrome model chromophore and a comparison with biliverdin dimethyl ester (**4**).[2] The influence of the difference between **3** and **4** on the photophysical and photochemical behavior of the bilatrienes has been a matter for speculation.[1,3] It has been shown that the saturation in ring A induces a pronounced reactivity in the 4,5 double bond, resulting, for example, in a thermally reversible photodimerization[4] and in a reversible, photochemically assisted nucleophilic addition at C-5 in the case of octaethyl A-dihydrobilatriene.[5]

We have shown previously, by using various spectroscopic techniques, that at low concentrations two families of conformers coexist in the solutions of biliverdin dimethyl ester (**4**) in organic solvents.[6,7] The helically coiled species, the most abundant in most of the solvents,[8] is characterized by a large D_{UV}/D_{VIS} ratio (the ratio of the transition dipole moments of the UV and visible absorption bands), a large Stokes shift, relatively broad fluorescence and fluorescence-excitation bands in the visible region, a short-lived (ca. 20 ps) excited singlet state, and a relatively large solvent-induced circular dichroism. The stretched species, on the contrary, is inherently more rigid, with a fluorescence lifetime on the order of 1.4 ns, a narrower and more structured fluorescence emission and excitation spectrum with a small Stokes shift, a smaller D_{UV}/D_{VIS} ratio, the visible fluorescence maximum at shorter wavelength, and a small solvent-induced circular dichroism. We also concluded that the *Z*-syn geometry within the A/B and C/D partial structures of **4** is retained in all these forms and that any stretched conformation adopts one of the several possible geometrical arrangements around the central C-10 bridge. Rotations around C-10, as well as intra- and intermolecular NH proton transfers, are the most important channels for radiationless deactivation of the excited coiled and stretched forms of **4**.[9,10]

We report now the results of a study of the photophysical and photochemical properties of phycocyanobilin dimethyl ester (**3**) (the diester **3** was preferred to the diacid **2** in view of the more convenient purification procedures and better solubility, and because comparison with **4** is straightforward). The self-sensitized photooxidation of **3** has been established both by detection of the infrared emission of $O_2(^1\Delta_g)$ upon steady-state and pulsed excitation of the bilatriene and by isolation of the reaction products. It constitutes the first evidence for excited triplet state formation of a bilatriene by intersystem crossing. The reaction of $O_2(^1\Delta_g)$ with the C-4 double bond and the reaction of the intermediate product with another molecule of **3**, again at the C-4 double bond, confirm that saturation of ring A selectively activates the adjacent C-4 double bond under oxidizing conditions.[5] The resulting peroxide is an interesting, stable product from the point of view of the types of compounds that can be obtained in biological media after exposure to $O_2(^1\Delta_g)$, e.g., in the case of photodynamic action.[11] The study of the influence of solvent, concentration, and excitation wavelength on the kinetics of photooxidation leads to a correlation of the photooxidation and photoisomerization of **3** (detected by laser-induced optoacoustic spectroscopy) with the various forms of the compound present in solution (coiled and stretched monomers plus aggregates, analogous to the case of **4**; detected by fluorescence emission and excitation spectroscopy). The results converge on a comprehensive picture of the photoexcited-state properties of the naturally occurring A-dihydrobilatrienes.

Experimental Section

Materials and Methods. Triethylamine (Merck) was distilled before use, trifluoroacetic acid (Merck) and ethanethiol (Merck, zur Synthese (z.S.)) were used as received. Polystyrene-bound rose bengal B (ca. 0.3 mmol/g resin), 1,3-dibromobenzene (purum), and 1,4-diazabicyclo-[2.2.2]octane were from Fluka, and gasses and gas filters from Messer Griesheim. All solvents were from Merck (zur Analyse (z.A.) quality) unless specified otherwise. For chromatography, the toluene was technical grade; for photochemical work, it was z.A. In every case it was chromatographed over basic Al_2O_3 prior to use. Sample solutions were either degassed by three freeze–pump (10^{-3} Pa)–thaw cycles or saturated with argon, air, or oxygen.

Electronic absorption spectra were measured with Perkin-Elmer 356 and 320 spectrophotometers. The absorption maxima were used to determine the ratio of the transition dipole moments for the UV and visible absorptions, D_{UV}/D_{VIS}.

Corrected fluorescence and fluorescence excitation spectra were obtained with a computer-controlled Spex-Fluorolog spectrometer.[12] For $A < 0.05$, cuvettes with a 1-cm optical pathlength were used. For more concentrated solutions, front-face fluorescence detection was employed with triangular cuvettes (Hellma, Müllheim). Fluorescence quantum yields were determined with cresyl violet as a reference ($\Phi_f = 0.54$ in methanol[13]). The integrated areas of the emission spectra of solutions of **3**, its protonated form, $3H^+$, and the thioethanol adducts, **5**, were compared with that of a cresyl violet solution at matched absorbances ($A \pm 0.006$ at $\lambda^{exc} = 640$ nm).

(2) Braslavsky, S. E.; Holzwarth, A. R.; Schaffner, K. *Angew. Chem., Int. Ed. Engl.* **1983**, *22*, 656–674. Schaffner, K. In *Neonatal Jaundice: New Trends in Phototherapy*; Rubaltelli, F. F., Jori, G., Eds.; Plenum Press: New York, 1984; pp 125–139.
(3) Rüdiger, W. *Struct. Bonding* **1980**, *40*, 101–140.
(4) Scheer, H.; Krauss, C. *Photochem. Photobiol.* **1977**, *25*, 311–314.
(5) Krauss, C.; Bubenzer, C.; Scheer, H. *Photochem. Photobiol.* **1979**, *30*, 473–477.
(6) Braslavsky, S. E.; Ellul, R. M.; Weiss, R. G.; Al-Ekabi, H.; Schaffner, K. *Tetrahedron* **1983**, *39*, 1909–1913.
(7) Al-Ekabi, H.; Tegmo-Larsson, I.-M.; Braslavsky, S. E.; Holzwarth, A. R.; Schaffner, K. *Photochem. Photobiol.* **1986**, *44*, 433–440.
(8) Falk, H.; Kapl, G.; Müller, N. *Monatsh. Chem.* **1983**, *114*, 773–781.
(9) Braslavsky, S. E.; Al-Ekabi, H.; Pétrier, C.; Schaffner, K. *Photochem. Photobiol.* **1985**, *41*, 237–246.
(10) Holzwarth, A. R.; Wendler, J.; Schaffner, K.; Sundström, V.; Sandström, A.; Gillbro, T. *Isr. J. Chem.* **1983**, *23*, 223–231. See also: Holzwarth, A. R.; Wendler, J.; Schaffner, K.; Sundström, V.; Sandström, A.; Gillbro, T. In *Picosecond Chemistry and Biology*; Doust, T. A. M., West, M. A., Eds.; Science Reviews: Northwood, 1983; pp 82–107.
(11) See, for example, contributions to *J. Photochem. Photobiol. B: Biology* **1990**, *6*, 1–196.
(12) Holzwarth, A. R.; Lehner, H.; Braslavsky, S. E.; Schaffner, K. *Liebigs Ann. Chem.* **1978**, 2002–2017.
(13) Magde, D.; Brannon, J. H.; Cremers, T. L.; Olmsted, J., III *J. Phys. Chem.* **1979**, *83*, 696–699.

The basic setup for the recording of **laser-induced optoacoustic spectra (LIOAS)** has already been described.[14] The equipment consists essentially of an Nd:YAG-pumped dye laser (JK Lasers system 2000, Rugby, U.K.) generating 15-ns pulses, and a piezoelectric detector equipped with a polyvinylidene difluoride (PVF_2)[14c] film, which monitors the acoustic waves generated by the radiationless processes in the sample. Rhodamine 6G and B, DCM, and Pyridine 1 (Lambda Physik, Göttingen, or Radiant Dyes-Chemie, Wermelskirchen) were used as laser dyes to cover the wavelength range 550–730 nm. The signals from the piezoelectric detector were treated by a homemade low-gain impedance converter, and after further amplification (Comlinear E 103A, 20 dB, DC-150 MHz, Transtech Hochfrequenztechnik, Hamburg), fed to a Biomation 8100 transient recorder (Gould Electronics, Seligenstadt) with a 10-ns sampling interval. Data acquisition and handling were performed with a PDP11/04-microVAX computer system. As calorimetric references, solutions of $CoCl_2$ and $CuCl_2$ in the same solvent and measured under the same conditions were used. $CoCl_2$ was used as received from Merck (z.A.), and $CuCl_2$ (Merck, z.A.) was recrystallized. The laser energy was varied with neutral-density filters and measured with a calibrated beam splitter and a pyroelectric energy meter (Rj-7100 and RjP-735, Laser Precision Corp., Polytech, Waldbronn). Various excitation-beam diameters in the cuvette, affording different effective acoustic transit times, $\tau'_a = 2R/v_a$ (R = Gaussian radius of the laser beam, i.e., the width at $1/e$ of the maximum intensity, v_a = sound velocity in the medium) were obtained by the use of calibrated pinholes and lenses with various focal lengths.

The **laser flash photolysis** equipment has also been described.[15] The energy-transfer method[16] was used in order to determine the triplet–triplet (T–T) absorption spectrum of **3**. Anthracene (Aldrich, recrystallized from ethanol, purity > 99.6% by gas chromatography) was used as a sensitizer. The 15-ns pulses from an excimer laser (EMG 101 MSC, Lambda Physik, Göttingen) at 308 nm (XeCl) served to excite the anthracene solutions.

$O_2(^1\Delta_g)$ emission under steady-state conditions was recorded with a home-built emission spectrometer with a Ge diode and signal recovery by lock-in amplification.[17] The solutions of **3** were circulated by means of a peristaltic pump (Abimed, Langenfeld) and irradiated at $\lambda > 475$ nm. In some cases, the solutions were degassed by freeze–pump–thaw cycles and measured without circulation. Discrete emission spectra were recorded between 1190 and 1340 nm at intervals of 10 nm and integration times of 50 s/point. The bandpass of the monochromator was 17 nm and the amplitude of the excitation beam was modulated at 33 Hz. $O_2(^1\Delta_g)$ was also detected by using 1,3-diphenylisobenzofuran as a chemical quencher. For this purpose, an IR-blocking filter (Schott KG5), a 515-nm cut-off filter (Schott), and an interference filter centered at 597 nm (Schott, 41% transmission, 13 nm FWHM) were used between the 450-W lamp (vide infra) and the cuvette containing 3.5 μM **3** and 10–50 μM diphenylisobenzofuran in aerated toluene. The solutions were continuously stirred and kept at 18 °C. The diphenylisobenzofuran bleaching, which was always <5%, was determined from the absorbance at 415 nm (ϵ_{415} = 23 100 M^{-1} cm^{-1} as derived from a conventional Beer–Lambert plot). The irradiation time was <20 min in order to minimize dark reactions, and the diphenylisobenzofuran solutions were always fresh. Actinometry was performed with Actinochrome N[18] (PTI, Tornesch/Hamburg). Bleaching of **3** was <1% in each measurement. The measurements were corrected for bleaching of diphenylisobenzofuran in the absence of **3** (20% of the bleaching in the presence of **3**).

The **$O_2(^1\Delta_g)$ quenching** constant for **3** was determined by laser-induced time-resolved phosphorescence detection as described.[17,19] The experimental decay measurements were corrected for an instrumental response decay of ca. 4 μs. *meso*-Tetraphenylporphine (Aldrich, purified following the method of Barnett et al.[20]) in benzene and hematoporphyrin (Sigma Chemie, Deisenhofen) in trifluoroacetic acid containing carbon tetrachloride were used as $O_2(^1\Delta_g)$ sensitizers. *meso*-Tetraphenylporphine was excited at 420 nm (laser dye Stilbene 3 pumped by the 308-nm ouput of an XeCl excimer laser, Lambda Physik), hematoporphyrin at 560 nm (Rhodamine 6G), and **3** at 600 nm (Rhodamine B, all laser dyes from Lambda Physik).

Mass spectra were measured by one of four methods: (i) Electron bombardment ionization (EI) with 70 eV was performed with Finnigan MAT 311A (for $M^+ < 900$) and 8230 spectrometers (for $M^+ > 900$). (ii) Chemical ionization (DCI) with NH_4^+ was carried out with the same equipment. (iii) For fast-atom bombardment (FAB)[21] with a double-focusing spectrometer VG 7070E, the samples were dissolved in a matrix of 2-nitrophenyl octyl ether. The FABs were conducted with Ar or Xe atoms. (iv) Resonance-enhanced multiphoton ionization (REMPI) with a reflection-time-of-flight (RETOF) mass spectrometer[22] was performed in order to establish the molecular weight of the thermally very labile peroxides **8–10**, ionization wavelength 272 nm, resolution $M/\Delta M$ = 6000.

The **NMR spectra** (^1H NMR and ^{13}C NMR) were run on WH-90, WH-270, and AM-400 (400 MHz for ^1H and 100.6 MHz for ^{13}C) spectrometers. The correlated spectroscopy (COSY) 2D NMR spectra were measured on the latter with degassed sample solutions. Chloroform-d_1 and dichloromethane-d_2 (Merck, Darmstadt) were chromatographed on Al_2O_3 before use. Chemical shifts are given in δ values relative to tetramethylsilane; abbreviations: m, multiplet; q, quartet; t, triplet; d, doublet; s, singlet; br, broad.

IR spectra were measured with Perkin-Elmer PE 257 and 580 spectrometers. Abbreviations: vw, very weak; w, weak; m, medium; s, strong; vs, very strong; br, broad; sh, shoulder.

Analytical Chromatography. High-performance liquid chromatography (HPLC): Perkin-Elmer System 3 with an LC-55 spectrophotometric detector (368 and 335 nm) and silica gel (Kieselgel 60, grain size 5–7 μm, Merck) columns (0.46 × 15 cm and 0.46 × 20 cm); solvent systems (A) chloroform/*n*-heptane/methanol = 10/80/0.5, (B) = 15/85/0.5, and (C) = 40/60/0.8. Thin-layer chromatography (TLC): Merck glass plates (20 cm) covered with silica gel (Kieselgel 60 F_{254}, 0.25 mm); solvent mixtures (A) chloroform/methanol/acetic acid = 9/1/0.01, (B) toluene/methanol/acetone = 2/1/1, (C) chloroform/ethyl acetate = 5/1; (D) toluene/ethanol/ethyl acetate = 20/1/1; spotting reagents (E) iodine, (F) $NaMnO_4$, (G) Dragendorff reagent according to Munier (Merck 120), (H) Dragendorff reagent according to Munier and Macheboeuf (Merck 121), (I) 2.5 g of molybdate phosphoric acid and 1 g of $Ce(SO_4)_2$ in 100 mL of 6% H_2SO_4, (K) 1 g of vanillin in 100 mL of concentrated H_2SO_4.

Preparative Chromatography. Merck plates with a layer thickness of either 1 mm (20 × 20 cm silica gel 60 F_{254}, with a concentration zone of 4 × 20 cm) or 2 mm (without concentration zone), using automatic seeding with an Autoliner (Desaga, Heidelberg), and silica gel 60 (grain size 40–63 μm) Lobar (Merck) A (240–10), B (310–25), and C (440–37) columns with a Duramat pump (pressures up to 7 bar) were employed. The eluents were deaerated, and saturated with and maintained under argon during chromatography. Short silica gel (Merck, either HF_{254} or H, grain size 10–40 μm) columns were used for final product purification.

Melting points were determined with a Reichert microscope (Kofler).

Phycocyanobilin Dimethyl Ester (3). The diacid phycocyanobilin (**2**) was extracted from spray-dried *Spirulina geitleri* algae (Winfried Behr, Bonn) according to Scheer[23] and esterified either by heating with 14% BF_3 in CH_3OH for 3 min[24,25] or by reacting in CH_3OH/concentrated H_2SO_4 (50/1) at 0 °C for 14 h. In each case the product was chromatographed over a type C column with toluene/ethanol/ethyl acetate = 100/1/1 at 5 bar pressure. Purity 97% by HPLC (solvent mixture A); yields ca. 3–4%; identification by comparison of the UV-vis (ϵ^{368}_{max} = 43 000, ϵ^{600}_{max} = 16 600 M^{-1} cm^{-1} in toluene, determined for four separately prepared concentrations), IR, MS, and ^1H NMR spectra with literature data.[24-27] Recrystallization from $CHCl_3/CH_3OH$ afforded samples of

(14) (a) Heihoff, K.; Braslavsky, S. E. *Chem. Phys. Lett.* **1986**, *131*, 183–188. (b) Heihoff, K.; Braslavsky, S. E.; Schaffner, K. *Biochemistry* **1987**, *26*, 1422–1427. (c) Braslavsky, S. E.; Heihoff, K. In *Handbook of Organic Photochemistry*; Scaiano, J. C., Ed.; CRC Press: Boca Raton, FL, 1989; Vol. I, pp 327–355.

(15) Ruzsicska, B. P.; Braslavsky, S. E.; Schaffner, K. *Photochem. Photobiol.* **1985**, *41*, 681–688. Armendia, P. F.; Ruzsicska, B. P.; Braslavsky, S. E.; Schaffner, K. *Biochemistry* **1987**, *26*, 1418–1422.

(16) Bensasson, R.; Land, E. J. *Trans. Faraday Soc.* **1971**, *67*, 1904–1915.

(17) Nonell, S.; Aramendia, P. F.; Heihoff, K.; Negri, R. M.; Braslavsky, S. E. *J. Phys. Chem.* **1990**, *94*, 5879–5883.

(18) Brauer, H.-D.; Schmidt, R.; Gauglitz, G.; Hubig, S. *Photochem. Photobiol.* **1983**, *37*, 595–598. Schmidt, R.; Brauer, H.-D. *J. Photochem.* **1984**, *25*, 489–499.

(19) Valduga, G.; Nonell, S.; Reddi, E.; Jori, G.; Braslavsky, S. E. *Photochem. Photobiol.* **1988**, *48*, 1–5.

(20) Barnett, G. H.; Hudson, M. F.; Smith, K. M. *J. Chem. Soc., Perkin Trans. 1* **1975**, 1401–1403.

(21) Devienne, F. M.; Roustan, J.-C. *C. R. Séances Acad. Sci., Sér. B* **1976**, *283*, 397–399. Barber, M.; Bordoli, R. S.; Sedgwick, R. D.; Tyler, A. N. *J. Chem. Soc., Chem. Commun.* **1981**, 325–327. Barber, M.; Bordoli, R. S.; Sedgwick, R. D.; Tyler, A. N. *Biomed. Mass Spectrom.* **1982**, *9*, 208–214.

(22) Grotemeyer, J.; Boesl, U.; Walter, K.; Schlag, E. W. *Org. Mass. Spectrom.* **1986**, *21*, 645–653.

(23) Kufer, W.; Scheer, H. *Hoppe-Seyler's Z. Physiol. Chem.* **1979**, *360*, 935–956. Scheer, H. In *Techniques in Photomorphogenesis*; Smith, H., Holmes, M. G., Eds.; Academic Press: London, 1984; pp 227–256.

(24) Cole, W. J.; Chapman, D. J.; Siegelman, H. W. *Biochemistry* **1968**, *7*, 2929–2935.

(25) Beuhler, R. J.; Pierce, R. C.; Friedman, L.; Siegelman, H. W. *J. Biol. Chem.* **1976**, *251*, 2405–2411.

(26) Schram, B. L.; Kroes, H. H. *Eur. J. Biochem.* **1971**, *19*, 581–594.

(27) Gossauer, A.; Hirsch, W. J. *Liebigs Ann. Chem.* **1974**, 1496–1513.

(28) Gossauer, A.; Hinze, R.-P.; Kutschan, R. *Chem. Ber.* **1981**, *114*, 132–146.

3 with a purity of >99.9% (HPLC), which were used for analytical irradiations, photophysical measurements, and the recording of the O_2-($^1\Delta_g$) IR emission. The neutral form of 3 was stabilized in CH_3OH with 10 mM $N(C_2H_5)_3$. The protonated form was studied in 2.5 mM CF_3CO_2H (CH_3OH).

(3*S*,3′*R)- and (3*S*,3′*S**)-3,3′-Dihydro-3′-thioethoxyphycocyanobilin Dimethyl Esters (5).** (The configurational assignments are based on a comparison with the data for **6**.) To a solution of **3** (38.2 mg, 0.057 mmol) in 1 mL of C_2H_5SH was added some *p*-toluenesulfonic acid. After stirring for 5 h at room temperature under Ar, the reaction mixture was poured into 30 mL of H_2O and extracted with $CHCl_3$. The organic solvents were evaporated under vacuum at room temperature and further dried under vacuum for 24 h. Chromatography on three consecutive Lobar columns (A, B, and C) under ca. 5 bar with toluene/ethanol/ethyl acetate = 100/1/1 gave the following fractions: (i) 8.8 mg of (3′*S**)-**5**, 98% purity by HPLC (solvent A); mp 139–140 °C; UV/vis λ_{max} [CH_3OH + 10 mM $N(C_2H_5)_3$] 345 (ε 26690), 580 nm (13835), [CH_3OH + 10 mM CF_3CO_2H] 345 (22275), 640 nm (26980); IR ($CHCl_3$) 2910 (m), 2850 (w), 1730 (s), 1690 (m), 1630 (m), 1600 (m), 1590 (sh), 1490 (w), 1450 (m) cm^{-1}; ^1H NMR ($CDCl_3$/270 MHz) δ 1.08 (t, $^3J_{18',18''}$ = 7.5 Hz, CH_3-18″), 1.21 (d, $^3J_{3',3''}$ = 6.75 Hz, CH_3-3″), 1.29 (t, ^3J = 8 Hz, SCH_2CH_3), 1.30 (d, $^3J_{2,2'}$ = 7.5 Hz, CH_3-2′), 2.00 (s, CH_3-7′), 2.08 (s, CH_3-13′), 2.11 (s, CH_3-17′), 2.30 (q, CH_2-18′), 2.53 (t, two α-CH_2 + br, CH-2), 2.63 (q, SCH_2CH_3), 2.90 (m, two β-CH_2), 3.09 (dd, $^3J_{2,3}$ = 5.25 Hz, $^3J_{3,3'}$ = 3.09 Hz, CH-3), 3.25 (m, CH-3′), 3.65, 3.67 (2 s, two CO_2CH_3), 5.44 (s, CH-5), 5.96 (s, CH-15), 6.65 (s, CH-10); MS (EI, 230 °C) *m/e* (rel intensity) 678 (16), 676 (94, M^+), 615 (base peak), 586 (85), 492 (13), 313 (80).

(ii) After further chromatography of this fraction on two silica gel columns with toluene/ethanol/ethyl acetate = 150/1/1, 6.9 mg of a mixture of 20% (by HPLC) (3′*S**)- and 80% (3′*R**)-**5** were obtained, mp 142–144 °C. Spectral data for (3′*R**)-**5**: ^1H NMR ($CDCl_3$/270 MHz): δ 1.07 (t, $^3J_{18',18''}$ = 7.5 Hz, CH_3-18″), 1.24 (t, ^3J = 7.5 Hz, SCH_2CH_3), 1.25 (d, $^3J_{3',3''}$ = 7.16 Hz, CH_3-3″), 1.40 (d, $^3J_{2,2'}$ = 6.75 Hz, CH_3-2′), 2.00 (s, CH_3-7′), 2.09 (s, CH_3-13′), 2.10 (s, CH_3-17′), 2.29 (q, CH_2-18′), 2.53 (t, two α-CH_2 + br, CH-2), 2.59 (q, SCH_2CH_3), 2.91 (m, two β-CH_2), 3.01 (dd, $^3J_{2,3}$ = 4.9 Hz, $^3J_{3,3'}$ = 3.8 Hz, CH-3), 3.17 (m, CH-3′), 3.66, 3.67 (s, two CO_2CH_3), 5.74 (s, CH-5), 5.96 (s, CH-15), 6.64 (s, CH-10); MS (DCI) *m/e* (rel intensity) 677 (base peak, M^+ + 1), 615 (36).

(iii) Mixture of **3** (30%), (3′*R**)- and (3′*S**)-**5** (25%), and *rac*-3′-thioethoxymesobiliverdin dimethyl ester (**11**, 45%). Spectral data for **11**: MS (EI, 230 °C) *m/e* (rel intensity) 674 (51, M^+), 613 (49), 313 (base peak); ^1H NMR ($CDCl_3$/270 MHz) δ 1.06 (t, CH_3-18″), 1.29 (t, SCH_2CH_3), 1.66 (d, $^3J_{3',3''}$ = 7.1 Hz, CH_3-3″), 1.89 (s, CH_3-2′), 2.07, 2.09, 2.10 (3 s, CH_3-7′, -13′, -17′), 2.30 (q, CH_2-18′), 2.53 (t, two α-CH_2), 2.62 (q, SCH_2CH_3), 2.90 (t, two β-CH_2), 3.66, 3.67 (2s, CO_2CH_3), 4.18 (q, CH-3′), 5.88 (s, CH-15), 6.44 (s, CH-5), 6.74 (s, CH-10).

Photophysical measurements were carried out only with (3′*S**)-**5**.

(3*S,3′*R**)- and (3*S**,3′*S**)-3,3′-Dihydro-3′-methoxyphycocyanobilin Dimethyl Esters (6).**[24] The 3′-diastereoisomers were prepared by doubling the reaction time of the esterification procedure of **2**.[24] Repeating column chromatography with petroleum ether/acetone 10/1 → 6/1 and chloroform/*n*-heptane/methanol 100/100/1 afforded (3′*R*)-**6** (97% purity by HPLC, solvent system B) and (3′*S*)-**6** (90%); identification of the two products was by comparison of the spectra with literature data.[29]

Irradiation of 3. Prior to the preparation of the sample solutions the solvent was degassed by sonication and flushing for 30 min either with Ar (99.996%, "oxygen-poor" condition) or with O_2. **3** was then added and the concentration was determined by absorption. The solution was then either further equilibrated for 10 min with Ar or O_2 or degassed by three freeze–pump–thaw cycles. All handling of the solutions was carried out under dim green light at 18 ± 1 °C.

For the analytical irradiations, the beam of a 450-W Xe lamp (XBO 450) was passed through a water filter and appropriate interference filters [λ_{max}/nm (FWHM/nm) = 360 (8.5), 532 (12.4), 545 (12), 577 (12), 597 (13), 626 (11.5), 643 (10.6); Schott, Zwiesel] and focussed onto a cuvette of either a 1-cm or 1-mm pathlength, depending on the concentration of the solution. In order to determine the quantum yield, the radiant power arriving at the cuvette was measured by recording with a 550-2 Photometer (EG&G Electrooptics Division) the power (>99%) reflected by a mirror set in place of the sample. The values for the total power in the cuvette for the various wavelengths were as follows: 577 nm, 3.33 mW; 597 nm, 3.75 mW; 626 nm, 3.71 mW; 643 nm, 3.07 mW.

Absolute quantum yields were determined by monitoring both products and bleaching of **3** by HPLC (solvent mixture C, response calibrated with **3** and the products) after evaporation of the solvent and dissolution of the residue in $CHCl_3$. Since the absorbance of **3** varied by up to 30% during irradiation, an average of initial and final absorbance was used for the calculation (provided the absorbance change was linear with time).

The relative quantum yields at the different excitation wavelengths and solvents were determined by the rate of photochemical conversion measured by difference absorption.

The time dependence of product formation in oxygen-poor toluene solutions of 1.2×10^{-5} M **3** was monitored by HPLC (solvent system C) over a period of 5–360 min irradiation time (λ^{exc} 577 nm).

For preparative purposes, the toluene solutions of **3** (15–20 mg in 100 mL) were irradiated for 17 h with the output of a 125-W Hg arc filtered through a cut-off filter (λ > 590 nm). The combined products of 5–6 runs (totalling the equivalent of 75–120 mg of **3**) were chromatographed through three connected columns (B plus 2 × C) with toluene/ethanol/ethyl acetate = 100/1/1 (6–7 mL/min). The products (purity 70–80%), repeatedly rechromatographed until a purity of 97% was obtained by HPLC (solvent system C), were (i) a mixture of **3** and its 3,3′-*Z* diastereoisomer[29] (7% yield) and (ii) 2-ethyl-3,7,13-trimethyl-8,12-bis(carbomethoxyethyl)-14-formyltripyrrin-1(15*H*)-one[30] (**7**, 11% yield of converted **3** + 3,3′-*Z* diastereoisomer): mp 168–169 °C; UV/vis λ_{max} ($CHCl_3$) 323 (28100), 508 (17500), 540 nm (17000); IR ($CHCl_3$) 3380 (w), 2960 (m), 2932 (m), 2860 (w), 1732 (s), 1710 (vs), 1645 (s), 1600 (m), 1460 (m), 1440 (m), 1392 (m), 1360 (m), 1170 (m), 1090 (m) cm^{-1}; for ^1H and ^{13}C NMR, see Tables I and II, respectively; MS (EI, 230 °C) *m/e* (rel intensity) 507 (base peak, M^+), 492 (5), 478 (10), 475 (81), 448 (12), 434 (45), 420 (18), 360 (36), 346 (12), 332 (22), 225 (7), 59 (32); (FAB, Ar) *m/e* 507 (M^+).

(iii) Bis-5,5′-phycocyanobilyl 4,4′-peroxides **8–10** were the third set of products, mp dec >150 °C. Spectral data for **8**: UV/vis λ_{max} ($CHCl_3$) 327 (55400), 570 nm (49500); IR ($CHCl_3$) 3340 (w), 2960 (m), 2935 (m), 2860 (w), 1730 (s), 1705 (m), 1665 (m), 1632 (w), 1602 (m), 1458 (w), 1440 (m), 1397 (w), 1170 (m), 1095 (m) cm^{-1}; ^1H NMR, see Table I and Figure 8; ^{13}C NMR, see Table II; MS (FAB, Xe) *m/e* 1260 (M^+, calcd $C_{70}H_{84}O_{14}N_8$ 1260.6107), 983 (base peak), 982; (REMPI-RETOF) *m/e* (rel intensity) 1260.61 (base peak), 1228 (48), 982, 614; (EI, 280 °C) *m/e* 982 (base peak), 684, 670. **9**: UV/vis λ_{max} (toluene) 329 (42300), 578 nm (37300); IR ($CHCl_3$) and MS (FAB, Xe) very similar to the spectra of **8**; ^1H NMR see Table I. **10**: UV/vis λ_{max} (toluene) 329 (40200), 569 nm (34800); IR ($CHCl_3$) and MS (FAB, Xe) very similar to the spectra of **8**.

Comparison of Direct and Triplet-Sensitized Irradiations of 3. Three-milliliter solutions of 2.4×10^{-5} M **3** (i) in aerated toluene, (ii) in aerated toluene containing 2 mg of polystyrene-bound rose bengal B, (iii) in aerated toluene containing 2 mg of the polystyrene-bound sensitizer and diazabicyclooctane (≥200 mM), and (iv) in oxygen-poor toluene were irradiated with λ^{exc} = 526 nm for 2 h. For product analysis by HPLC (condition C, λ^{obsd} = 615 nm) at 30-min intervals, aliquots of the solutions were withdrawn and the samples containing polymer suspensions were filtered. The consumption of **3** with time was linear for all four samples in the relative order (ii) > (i) > (iii) > (iv).

Results

Fluorescence Spectroscopy. At low concentrations of **3** (4×10^{-6} M) the fluorescence spectrum is composed of two bands, a narrow one at 633 nm and a broader one around 680 nm (Figure 1b,c). The intensity ratio of the two bands depends on the excitation wavelength: the narrow band arises preferentially upon excitation at 340 nm, while the broader emission is favored at λ^{exc} = 400 and 580 nm (Figures 1 and 2). The latter is difficult to obtain separate from a third still broader emission band appearing at around 700 nm (Figure 1b), particularly upon excitation at 390 nm.

The form of the fluorescence spectra of **3** depends also on the concentration. At 10^{-6} M **3** the narrow band is more intense (Figure 3b), whereas at higher concentrations (≥10^{-5} M) the two broad bands around 680 and 700 nm predominate (Figure 3a).

The emission and excitation characteristics in toluene are similar to those in methanol shown in Figures 1–3, and so are the spectra of (3′*S**)-**5**.

In acidified solvents, the fluorescence and excitation spectra of $3H^+$ are red-shifted, and two species can be distinguished (spectra not shown) similar to the case of **3**. The responses to

(29) Weller, J.-P.; Gossauer, A. *Chem. Ber.* **1980**, *113*, 1603–1611.

(30) (a) Scheer, H.; Linsenmeier, U.; Krauss, C. *Hoppe-Seyler's Z. Physiol. Chem.* **1977**, *358*, 185–196. (b) Krauss, C. Doctoral Thesis, Universität München, Munich, Germany, 1980. Similar tripyrrones have been obtained also upon photochemical and dark oxidations of model bilindiones.

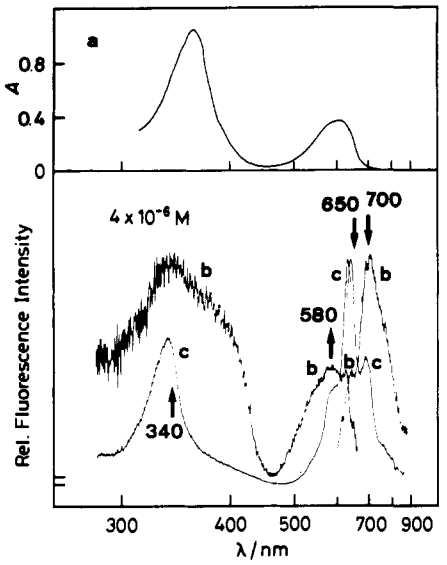

Figure 1. (a) UV/vis absorption spectrum of **3** in methanol + 10 mM triethylamine (no change with concentration observed). Corrected fluorescence and fluorescence excitation spectra of **3** in methanol: (b) λ^{exc} = 580 nm, λ^{em} = 700 nm; (c) λ^{exc} = 340 nm, λ^{em} = 650 nm.

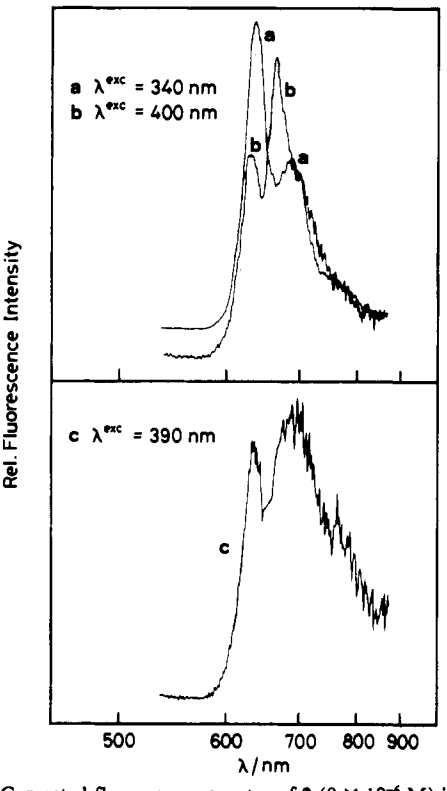

Figure 2. Corrected fluorescence spectra of **3** (8×10^{-6} M) in methanol + 10 mM triethylamine: Dependence on the excitation wavelength.

excitation wavelength and concentration parallel those exhibited by **3**.

The fluorescence quantum yields (Φ_f) in methanol are 2.0×10^{-3} for **3**, 2.5×10^{-3} for $3H^+$, and 4.2×10^{-3} for **5**. The fluorescence spectra of the peroxide **8** in methanol (2.5×10^{-5} M) showed an excitation-wavelength dependence similar to that exhibited by **3** and **5**. By excitation at 340 nm, a narrow emission band at λ^{em} = 631 nm is observed, while a broad emission centered at 636 nm results on excitation at 510 nm. The excitation bands are also different, depending on λ^{obsd} (spectra not shown). A Φ_f value of 1.99×10^{-3} at λ^{exc} = 500 nm was determined. These results are reminiscent of those of **3** and evidently also reflect a heterogeneous composition of conformers. A more detailed interpretation, however, is presently not warranted.

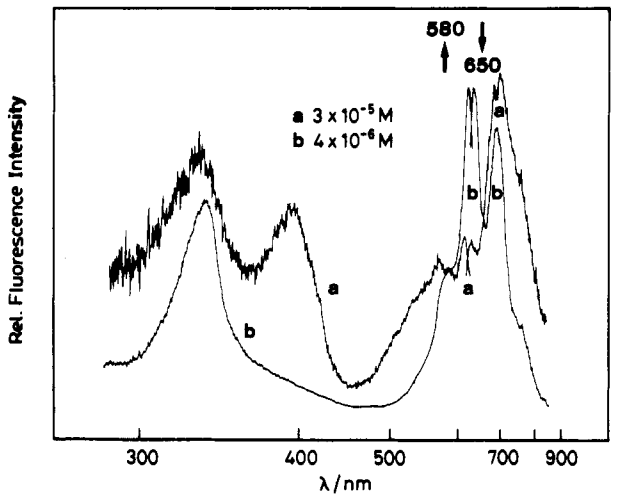

Figure 3. Corrected fluorescence and fluorescence excitation spectra of **3** in methanol + 10 mM triethylamine: Dependence on concentration. (a) Emission and excitation maxima of the mixture of stretched (λ^{em}_{max} = 633 nm, λ^{exc}_{max} = 377, 623 nm) and helically coiled conformers (λ^{em}_{max} ca. 680 nm, λ^{exc}_{max} 400, 582 nm). (b) Fluorescence and excitation of predominantly stretched conformers. Note in spectrum a the broadening of the fluorescence band at longer wavelengths by aggregates.

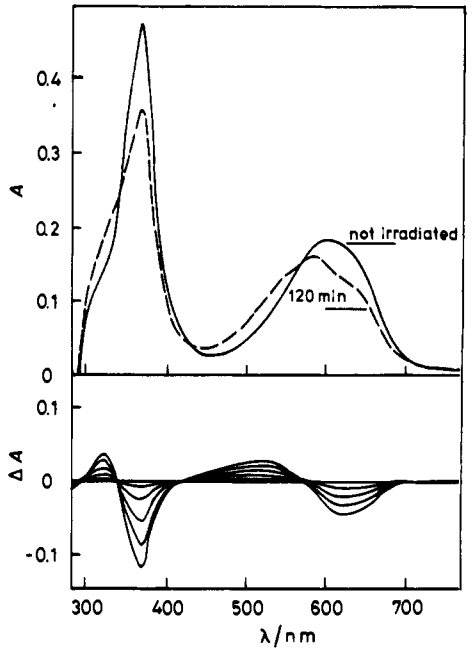

Figure 4. Irradiation of **3** under oxygen-poor conditions. Top: Absorption spectra of nonirradiated and 120-min-irradiated (λ^{irr} = 577 nm) toluene solutions of 10^{-5} M **3**. Bottom: Difference absorption spectra after 10, 30, 60, 90, and 120 min after irradiation.

Irradiation of Phycocyanobilin Dimethyl Ester (3). Figure 4 shows difference absorption spectra resulting from irradiation at λ = 577 nm of a 10^{-5} M argon-flushed ("oxygen-poor") solution of analytically pure **3** in toluene as a function of irradiation time. While the near-UV and red absorption maxima of **3** were bleached, two new bands appeared around the 320- and 500-nm regions. Similar difference spectra were obtained when **3** was irradiated under oxygen-poor conditions in methanol, benzene, dimethyl sulfoxide, and dimethyl ether (spectra not shown). The intensity of bleaching (ΔA_{bl}) at its maximum (610–620 nm, depending on the solvent) served to estimate the reaction yield under the various conditions. The linear region of the plots of $\Delta A_{bl}/A_0$ (A_0 = initial absorbance at λ_{max}) vs irradiation time (plots not shown) yielded the rate constants for the bleaching of **3**, k_{-3}. In thoroughly degassed solutions, neither bleaching nor the appearance of any new absorption bands was observed in the above solvents after 6 h of irradiation.

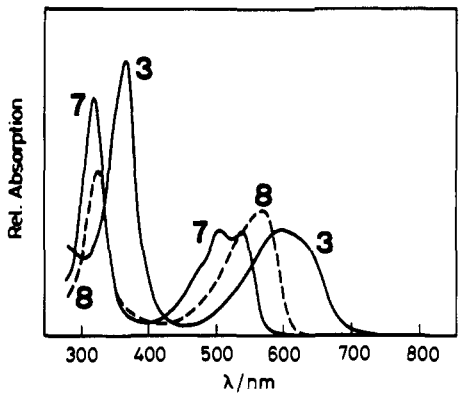

Figure 5. Absorption spectra of a ca. 10^{-5} M $CHCl_3$ solutions of **3**, **7**, and **8**.

Scheme II[a]

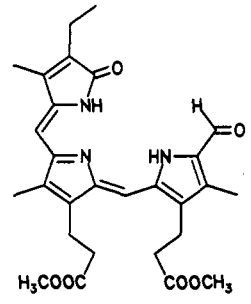

7

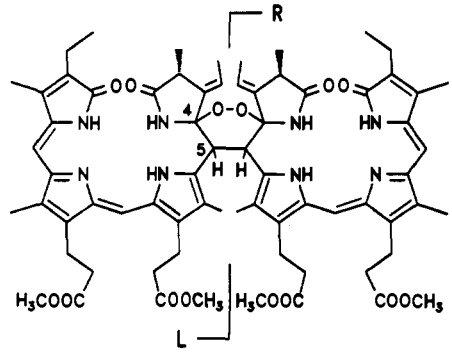

8, 9, 10

[a] Irradiation of **3** in oxygen-containing solution: Structure of products **7**–**10**.[32] The conformations are chosen arbitrarily; for the configurational assignments to C-3′, C-4, and C-5, see Scheme III and Discussion.

Preparative irradiation of **3** in oxygen-poor dilute toluene solutions afforded, besides **12**, the 3,3′-*Z* isomer of the starting material, four major products, **7**, **8**, **9**, and **10** in yields of about 11%, 5%, 1.5%, and 2%, respectively, (at ca. 93% conversion of starting material; the substantial percentage of unaccounted material is composed of products of lower molecular weights, which have not been further characterized). The time dependence of the formation of **7** and **8** showed these compounds (and by analogy also the stereoisomers of **8**, i.e. **9** and **10**) to be primary products. Product **7** was red, and **8**–**10** were violet. In Figure 5, the absorption spectra of **7** and **8** (the spectra of **8**, **9**, and **10** are very similar) are juxtaposed with the spectrum of **3**. The structure of the tripyrrolic aldehyde **7** (Scheme II) was identified by ^1H NMR, ^{13}C NMR, and EI mass spectroscopy comparisons with a product obtained previously by alkaline oxidation of the zinc acetate complex of **3**.[30]

Upon irradiation of aerated solutions of **3**, the violet products (**8**–**10**) were not formed; only **7** was observed. The difference absorption spectrum between irradiated and nonirradiated solutions showed a similar difference spectrum (Figure 4)—albeit with greater absorbance differences—as the run under oxygen-poor conditions in the same solvent.

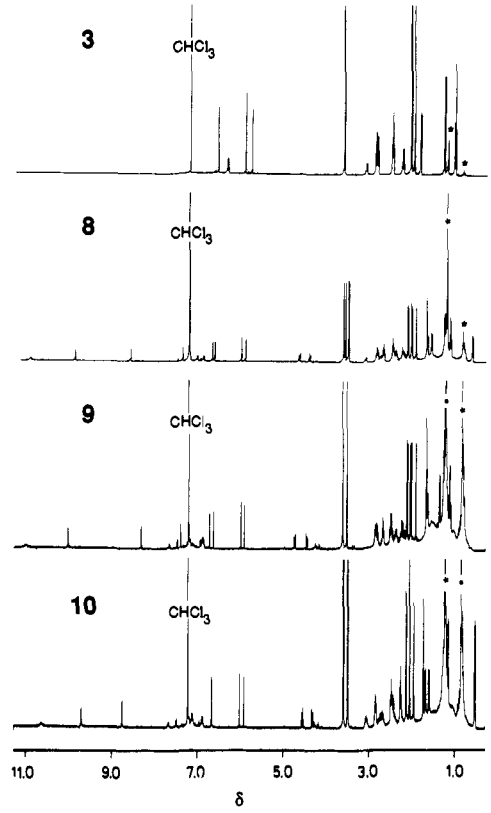

Figure 6. ^1H NMR spectra (400 MHz) of **3** (8.1×10^{-2} M, shown for comparison), **8** (1.5×10^{-2} M), **9** (7.5×10^{-3} M), and **10** (8.9×10^{-3} M) in $CDCl_3$; *, impurity signals due to solvent and silica gel.

Structure Elucidation of Product 8. The ^1H and ^{13}C NMR assignments were mostly based on comparisons with corresponding ^1H and ^{13}C NMR data for **3** and **4**[31] (assignments of the quaternary carbons linked to N by double bonds), and on analysis by ^1H–^1H homoscalar-correlated COSY 2D and ^{13}C–^1H heteroscalar-correlated NMR spectra (Tables I and II). The ^1H NMR spectrum of **8** (Figure 6) shows two sets of almost all signals of **3**. A molecular weight determination by REMPI–RETOF mass spectrometry gave a parent peak at *m/e* 1260.61 and another peak at 614, compatible with the composition of the bis(phycocyanobilyl) peroxide structure **8** and a fragment corresponding to **3**, respectively. Identical isotope distributions of the peaks around *m/e* 1260 (M^+) and 1228 ($M^+ - O_2$) identified the molecular ion as that of a peroxide. A strong support for the constitution of **8** can be derived from the base peak of mass 982 in the EI spectrum, which corresponds to a fragment formed by the loss of rings A^R and A^L and of O_2.

^1H NMR singlets at δ 7.42, 8.61, and 9.92 and a broad signal at δ 11.07 underwent an H/D exchange upon D_2O addition and were therefore assigned to four NH protons. Two more NH proton signals appeared at δ 10.02 and 10.41 upon cooling to 243 K. Evidently proton exchange in **8** is not as rapid as in **3**, which displays individual NH signals only at 213 K. At room temperature, merely a broad band (δ 7.5–9.0) for 1–2 N-bound protons of **3** could be discerned.

The $C\text{-}5^L$–$C\text{-}5^R$[32] linkage of the two phycocyanobilyl moieties was derived from the vicinal ^1H NMR coupling at these positions (doublets with ^3J = 13.6 Hz), and the peroxide bridge location

(31) Wray, V.; Gossauer, A.; Grüning, B.; Reifenstahl, G.; Zilch, H. *J. Chem. Soc., Perkin Trans. 2* **1979**, 1558–1567.

(32) The tetracyclic ring A–D "halves" of the bis(phycocyanobilyl) peroxide products are defined as left and right as depicted in the formulas of Scheme II, and references to and values for these "halves" are designated by the superscripts L and R, respectively.

Table I. ^{1}H NMR Data for **3** (3,3′-*E*), 3,3′-(*Z*)-Phycocyanobilin Dimethyl Ester (**12**), and the Photoproducts **7–10**

	chemical shift (upper line(s)) and signal multiplicity (bottom line; in parentheses coupling constants unless specified otherwise)[a]								
				8		**9**		**10**	
position	**3**	**12**[b]	**7**	left[c]	right[c]	left[c]	right[c]	left[c]	right[c]
CH_3-2′	1.32	1.25		0.64[d]	1.29[d]	1.29[d]	1.38[d]	0.54	0.54
	d (8.0)	d (8.0)		d (7.5)	d (7.5)	d (7.2)	d (7.2)	d (7.6)	d (7.6)
CH-2	3.14	2.8–3.1		3.11[d]	2.77[d]	2.82[d]	2.87[d]	3.03	3.13
	dq (2.0)	m		dq (2.0)	dq (2.0)	m	m	m	m
CH-3′	6.38	5.84		7.09[d]	6.90[d]	6.91	6.91	6.91	7.14
	dq (2.0)	m		dq (2.0)	dq (2.0)	m	m	dq (2.0)	dq (2.0)
CH_3-3″	1.88	2.08		1.60[d]	1.69[d]	1.66	1.69	1.70	1.62
	d (7.6)	dd (8.0)		d (6.8)	d (6.8)	d (7.2)	d (7.2)	d (7.0)	d (7.0)
CH_3-7′	2.02	2.04	2.31	1.72	1.98	1.69	1.94	1.75	1.97
	s	s	s	s	s	s	s	s	s
CH_3-13′	2.09		2.07	2.13	2.18	2.14	2.15	2.14	2.15
	s	2.12	s	s	s	s	s	s	s
CH_3-17′	2.11	s	2.10	2.05	2.08	2.05	2.07	2.07	2.07
	s		s	s	s	s	s	s	s
CH_3-18″	1.07	1.07	1.13	1.16[d]	1.15[d]	1.16	1.15	1.17	1.18
	t (8.0)	t (7.0)	t (7.6)	t (7.5)	t (7.5)	t (7.6)	t (7.6)	t (8.0)	t (8.0)
CH_2-18′	2.30	2.34	2.41	2.48[d]	2.42[d]	2.40	2.40	2.43	2.43
	q (8.0)	q (7.0)	q (7.6)	q (7.5)	q (7.5)	m	m	m	m
α-CH_2	2.53	2.4–2.7	2.54	2.24	2.24	2.23[d]	2.27[d]	2.27	2.27
	t (7.6)	m	t (7.5)	2.49	2.49	2.50[d]	2.53[d]	2.52	2.52
				2 m	2 m	2 t	2 t	2 m	2 m
β-CH_2	2.90	2.8–3.1	2.94	2.72	2.72	2.71	2.71	2.63[d]	2.81[d]
	t (7.6)	m	2.89	2.86	2.86	2.82[d]	2.85[d]	2.86	2.86
			2 t (7.5)	2 m	2 m	2 t	2 t	m	m
CO_2CH_3	3.65	3.68	3.63	3.53	3.54	3.56	3.56	3.51	3.53
	3.66	3.69	3.64	3.61	3.66	3.65	3.65	3.60	3.63
	2 s	2 s	2 s	2 s	2 s	2 s	2 s	2 s	2 s
CH-5	5.82	5.93[e]	9.79	4.68	4.43	4.77	4.49	4.57	4.33
	s	s	s	d (13.6)	d (13.6)	d (12.6)	d (12.6)	d (13.1)	d (13.1)
CH-10	6.60	6.72	6.78	6.64	6.69	6.66	6.76	6.69	6.78
	s	s	s	s	s	s	s	s	s
CH-15	5.97	6.00[e]	5.84	5.94	6.03	5.95	6.03	5.94	6.04
	s	s	s	s	s	s	s	s	s
NH	10.37	[g]	9.30						
	11.03		br (26 3[f])						
	11.03		11.38						
	3 br (21 3[f])		br (25 3[f])						
	7.42			7.43		7.27[h]			
	8.61			8.34		8.77			
	9.92			10.05		9.73			
	3 s (RT[f])			3 s (RT[f])		3 s (RT[f])			
	11.07			11.03		10.65			
	br (RT[f])			br (RT[f])		br (RT[f])			
	10.02			9.97		9.80			
	10.41			br (26 3[f])		10.32			
	2 br (24 3[f])			10.42		2 br (22 3[f])			
				br (24 3[f])					

[a] $CDCl_3$ solution; chemical shifts in δ values; coupling constants (^3J, hertz) in parentheses; for abbreviations see the Experimental Section. [b] Data from ref 26. [c] See ref 32. [d] Arbitrary assignment of the ^{1}H shifts (and the corresponding ^{13}C listed in Table II) to the left or right "halves" of the molecule. [e] Assignments interchangeable. [f] Temperature (Kelvin; RT = ambient temperature) in parentheses; H/D exchange with D_2O observed. [g] Value not reported. [h] Extrapolated from δ = 7.02 in CD_2Cl_2.

follows from the considerable upfield shifts that occur only for CH-2, CH_3-2′, CH-3′, CH-5, and CH_3-7′ on either or both "halves" (Table I). The CH-5^L–CH-5^R coupling corresponds, according to the Karplus relation, to torsion angles of either 0–15° or 160–180°. The latter angle avoids severe steric constraints and invokes a chair conformation for the peroxide ring with axial hydrogens at C-5^L and C-5^R, i.e., a thermodynamically favorable arrangement with the two bulky rings B^L and B^R in synclinal equatorial positions. On this basis the total number of possible diastereoisomeric arrangements of the four chiral carbons around the peroxide ring is reduced from an a priori 16 to the eight shown in Scheme III [a set of three independent chiral elements, viz. C-4^L, C-4^R, and C(5^L + 5^R)].

One of the CH_3-2′ groups exhibits the largest upfield shift of all (Δδ ca. 0.6 ppm from the second CH_3-2′ position which, in turn, agrees closely with the chemical shift of the corresponding methyls of **3**), which is only attributable to selective diamagnetic shielding by either ring B^L or B^R in the isomers a_1, a_2, b_1, and b_2. The second methyl, CH_3-2′^{L} in a_2 and b_2 and CH_3-2′^{R} in a_1 and b_1, should be out of range from the nearest ring-B current, thus justifying its unaltered signal position. The other structures of Scheme III do not account for any such differential shift: in a_3 and b_4, both methyls are out of range of the two ring currents, and in a_4 and b_3, both are equally as close to a ring B as compared to only one methyl in a_1, a_2, b_1, and b_2. The assignment of **8** to either a_1, a_2, b_1, or b_2 is compatible with the nuclear Overhauser (NOE) effects observed on the one hand, between one CH-5 (δ 4.43) and the N-bound protons of the A rings at δ 7.42 and 8.61 (3–4% NOE each) and, on the other hand, between the other CH-5 (δ 4.68) and the two CH-3′ protons (centered at δ 6.90 and 7.09, 10% NOE each). Such NOEs are to be expected only for a_1, a_2, b_1, and b_2. The results implicitly document that **8** is constituted of two units of **3** rather than representing a combination of one unit of **3** and one of **12**.

Structure of Products 9 and 10. Mass and ^{1}H NMR spectra (Figure 6, Table I) clearly demonstrated the diastereoisomeric

Table II. ^{13}C NMR Data for **3** and the Photoproducts **7** and **8**

	chemical shift (δ)/signal multiplicity[a]			
			8	
position	**3**	**7**	left[b]	right[b]
CH_3-2′	15.57/q		15.32/q[c]	16.67/q[c]
CH-2	37.92/d		40.14/d[c]	38.63/d[c]
CH-3′	122.82/d		125.98/d[c]	128.97/d[c]
CH_3-3″	14.89/q		14.61/q[c]	14.54/q[c]
CH_3-7′	9.64/q	8.57/q	8.38/q	8.59/q
CH_3-13′	9.73/q	9.89/q	9.46/q	9.60/q
CH_3-17′	9.26/q	9.45/q	9.63/q	9.86/q
CH_3-18″	12.99/q	13.19/q	13.39/q[c]	13.23/q[c]
α-CH_2	35.18/t	35.00/t	35.30/t[c]	35.28/t[c]
	35.25/t	35.05/t	35.34/t[c]	35.34/t[c]
β-CH_2	19.70/t	19.25/t	19.87/t[c]	19.82/t[c]
	19.86/t	19.85/t	20.61/t[c]	20.61/t[c]
			51.66/q[c]	51.68/q[c]
CH-5	87.33/d	177.95/d	41.71/d	44.70/d
CH-10	111.12/d	113.88/d	116.33/d	116.57/d
CH-15	96.14/d	95.18/d	97.18/d	98.85/d
$CC(N)O_2$			93.93/s	95.71/s
CO_2CH_3	51.66/q	51.74/q	51.57/q	51.57/q
C_{quart}	123.38/s	128.60/s	121.92/s[c]	122.49/s[c]
	131.15/s	130.03/s	125.98/s[c]	127.55/s[c]
	132.12/s	133.17/s	128.96/s[c]	129.53/s[c]
	132.23/s	133.23/s	131.71/s[c]	132.12/s[c]
	133.19/s		132.92/s[c]	133.22/s[c]
	133.72/s		133.99/s[c]	134.08/s[c]
	135.88/s	135.03/s	135.35/s[c]	135.60/s[c]
	136.98/s	136.47/s		
	141.27/s	139.85/s	139.70/s[c]	140.98/s[c]
	141.66/s	143.34/s	141.86/s[c]	143.57/s[c]
	145.63/s	146.40/s	143.37/s[c]	143.57/s[c]
	148.74/s	153.35/s	146.68/s[c]	147.81/s[c]
C=N	165.62/s	169.26/s	163.01/s	165.65/s
CO_2CH_3	173.13/s	172.95/s	172.92/s	172.98/s
	173.15/s	173.03/s	173.06/s	173.15/s
C(O)N (ring D)	173.29/s	171.28/s	171.13/s	173.56/s
C(O)N (ring A)	178.03/s		177.06/s	179.74/s

[a] See footnote *a* of Table I. [b] See ref 32. [c] Arbitrary assignment to the left or right "halves"; see footnote *d* of Table I.

relation of the three violet photoproducts **8–10**. FAB-MS gave average values of m/e = 1262–1263 for the parent peaks, with relative isotope peak ($M^+ + 1$) intensities of 77%, showing that each compound is composed of 70 carbon atoms. Identical fragmentation patterns substantiate the constitutional identity of all three products. The ^1H NMR analysis including the COSY proton sequences confirm the assignment.

Vicinal ^1H NMR coupling constants around 13 Hz show that the hydrogens at C-5^L and C-5^R are again both axial. The CH_3-2′ chemical shift positions are unchanged in **9**, whereas in **10** both methyls experience an upfield shift of the same order as one methyl in **8**. Structures a_3 and b_4 must therefore be considered for product **9**, while a_4 and b_3 are compatible with **10**. The experimental product ratio of 3/1/1.3 for **8/9/10** is reasonably close to the ratio 2/1/1 expected on the basis of the above structural assignments.

The C_2 symmetry of the structures a_3, a_4, b_3, and b_4 should per se be reflected in the ^1H and ^{13}C NMR spectra, which is not the case (Figure 6). This is readily explicable by the buildup of a photochromic equilibrium **3** $\rightleftarrows$ **12**,[29] prior to the peroxide formation, through *E,Z* photoisomerization of the C(-3)=C(-3′) bond within the laser flash duration of 15 ns.[33] Products **9** and **10** are therefore mixtures of 3,3′-*E,Z* isomers rather than products with equivalent left and right "halves".[34] Interestingly, the NOE data for **8** has ruled out a similar mixed origin of this product. It should be noted, furthermore, that the establishment of the photochromic equilibrium **3** $\rightleftarrows$ **12** under the irradiation conditions is compatible with the postulate that **9** and **10** are primary products of the photooxidation.

Scheme III[a]

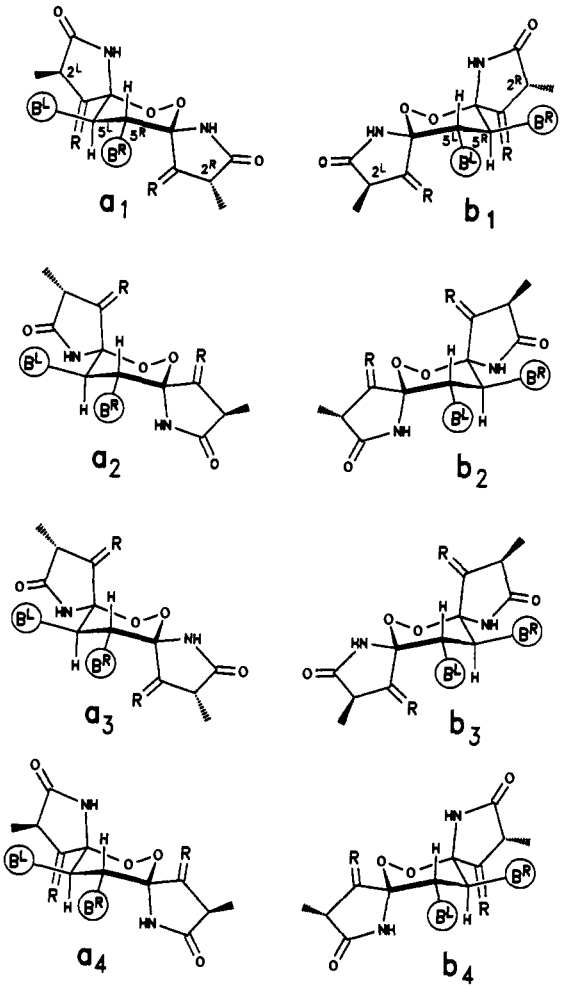

[a] Energy-minimized diastereoisomeric arrangements with axial hydrogens at C-5^L and C-5^R considered for the peroxide products **8–10**. The designations B^L and B^R refer here to rings B–D of the left and right molecular "halves", respectively. Note that the a–b pairs are mirror images only with respect to the four chiral centers of the peroxide ring. R = *E*- or *Z*-ethylidene group (see Results).

A definitive differentiation between the a- and b-type structures for **8–10** is presently not possible. In summary, then, the remaining possible structures are a_1, a_2, b_1, and b_2 for **8**, a_3 and b_4 for **9**, and a_4 and b_3 for **10**.

Determination of Reaction Quantum Yields. The quantum yields of the consumption of **3** and of product formation, determined from the linear part of the time dependence of the photochemical conversion in oxygen-poor toluene, were $\Phi_{-3} = (1.6 \pm 0.6) \times 10^{-4}$, $\Phi_7 = (1.2 \pm 0.6) \times 10^{-5}$, and $\Phi_8 = (4.7 \pm 2.7) \times 10^{-6}$ (λ^{exc} = 577 nm). The ratios Φ_7/Φ_{-3} ca. 0.08 and Φ_8/Φ_{-3} ca. 0.03 are similar to the corresponding values obtained by HPLC analysis of preparative irradiation, ca. 0.11 and ca. 0.05, respectively. The quantum yields of formation of **9** and **10** under the same conditions were ca. 1.5×10^{-6} and 2×10^{-6}. In aerated solutions, the quantum yield of photoconversion, Φ_{-3}, was larger by a factor of 3.

Dependence of the Photoconversion of 3 on Wavelength, Solvent, and Concentration. The relative quantum yields, Φ_{-3}, i.e., the k_{-3} values normalized to the absorbance by **3** and for the fluence at the excitation wavelength in oxygen-poor toluene (1.8×10^{-5} M) and methanol (1.8×10^{-5} M + 10 mM triethylamine), varied strongly with λ^{exc}, as shown in Figure 7 for toluene solution.

At λ^{exc} = 577 nm, k_{-3} was 5 times larger for toluene than for methanol. In acidic media, k_{-3} (of $3H^+$) was about 10 times

(33) A lifetime of about 20 ps is estimated for the singlet excited state on **3** on the basis of the close similarity of its fluorescence spectrum with that of **4**, which has a singlet lifetime τ_f ca. 25 ps at room temperature.[2,10]

(34) Another trivial reason for the lack of symmetry in the NMR spectra of **9** and **10** could be a heterogeneity of the two samples, viz. a inseparable mixture composed, in each case, of two products with equivalent "halves" with either the 3,3′-*E* or 3,3′-*Z* configuration.

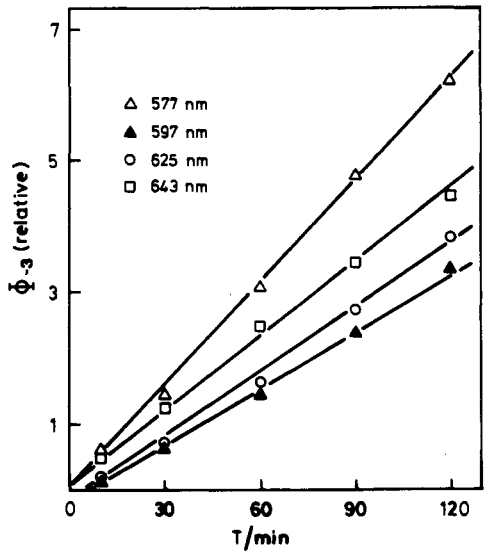

Figure 7. Influence of excitation wavelength on the time dependence of the photoconversion yield of **3** (1.8×10^{-5} M), Φ_{-3}, in oxygen-poor toluene solution, corrected for the fraction of light absorbed and for the light fluence at each λ^{exc}.

smaller than in the corresponding neutral solvents. Concentration had also a very marked effect. An almost linear increase of Φ_{-3} was found from 10^{-6} to 10^{-4} M **3** in oxygen-poor toluene solution, reflecting a square dependence. In aerated solutions, the effects of wavelength and concentration were similar to those in the oxygen-poor solutions.

Deuterium/Hydrogen Isotope Effect. The ratio of the k_{-3} values for aerated solutions (1.5×10^{-5} M **3**) at λ^{exc} = 577 nm was $k^{D}_{-3}/k^{H}_{-3} = 2 \pm 0.3$ for toluene-d_8/toluene (λ^{obsd} = 615 nm) and 9 ± 1 for methanol-d_4/methanol (λ^{obsd} = 610 nm).

Singlet Oxygen Sensitization of 3. In comparison to a parallel irradiation of **3** in an aerated toluene solution without added sensitizer, the consumption of **3** was accelerated in the presence of polystyrene-bound rose bengal, and it slowed down to a rate slower than in oxygen-poor toluene when diazabicyclooctane was added to the solution of **3** and sensitizer (data not shown).

Irradiation of (3*S,3′*R**)-3,3′-Dihydro-3′-methoxyphycocyanobilin Dimethyl Ester (6).** The irradiation (λ^{exc} = 526 nm) of an epimeric mixture of **6** in aerated toluene solutions caused bleaching of the absorption spectrum (λ_{max} = 340 and 586 nm), and a deuterium–hydrogen isotope effect of $k^{D}_{-3}/k^{H}_{-3} = 1.3$ was measured for toluene-d_8/toluene, all quite similar to the case of **3**. Two new product absorptions at 310 and 480–500 nm appeared upon these irrradiations. The difference absorption spectrum was quite similar to that of the analogous experiment with **3** (cf. Figure 4). A further characterization of the photoproduct(s) of **6** was not attempted.

Laser-Induced Optoacoustic Spectroscopy. For the analysis of the LIOAS signal, the amplitude of the first maximum was used, which is proportional to the energy absorbed by the sample, $E_0 \times (1 - 10^{-A})$, to the thermoelastic parameters of the solution, to geometrical parameters, and to α, the fraction of absorbed light energy dissipated as heat to the medium. The appropriate equations have been derived elsewhere.[35]

Absorbances of the sample solutions in the range of A = 0.04–0.3 were chosen for each excitation wavelength. Routinely, the linearity of the optoacoustic signal amplitude, H, with laser excitation energy, E_0, was checked in the range 1–20 μJ (corresponding to 0.03–30 photons per molecule). At $E_0 \leq 5$ μJ no change in absorbance was detected during the laser pulse. Absorption saturation and ground-state bleaching occurred only at the higher photon densities, especially with focused beams. This was also observed by monitoring the absorbance with an additional pyroelectric detector behind the sample cuvette.

The fraction α released within the time resolution of the experiment (= prompt heat dissipation) was determined from the ratio of the slopes of the energy-normalized signal amplitudes, H/E_0, (measured in the linear range of 1–5 μJ of energy dependence, data not shown) for sample and reference.[6] Table III lists the α values for **3** in methanol at concentrations $< 2.5 \times 10^{-5}$ M and $\tau_a' = 110$ ns as a function of excitation wavelength. The smallest α values (<1.0) were recorded in the 600–640-nm region, which coincides with the excitation maximum of the narrow lower wavelength emission band. Similar results were also obtained for $3H^+$ and the thioethoxy derivative **5**. Furthermore, there was no difference between degassed, oxygen-poor, and aerated solutions of **3** and **5**.

The dependence of the energy-normalized amplitude H/E_0 on $(1 - 10^{-A})$ is shown in Figure 8 for **3** and a reference sample. While the dependence is linear for the latter, it curves upward for **3** solutions of concentrations greater than 4×10^{-5} M. For ca. 6×10^{-5} M **3**, the α value reaches unity.

Table III. LIOAS: Dependence of Prompt Heat Dissipation (α) from Excited **3**, $3H^+$, and (3′*S**)-**5** on the Excitation Wavelength

3[a,b]		$3H^{+}$[a,c]		**5**[a,b]	
λ^{exc}/nm	α	λ^{exc}/nm	α	λ^{exc}/nm	α
550	1.0	640–650	0.8	550	1.0
600–620	0.7	690–710	0.6	585	0.8
640	0.8	735	0.8	620	0.8
660	1.0			630	1.0

[a] Methanol solutions, concentrations $< 2.5 \times 10^{-5}$ M. [b] Triethylamine added (10^{-2} M). [c] Trifluoroacetic acid added (2.5×10^{-3} M).

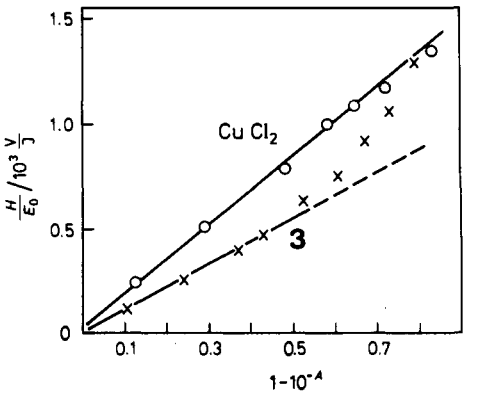

Figure 8. Dependence of the energy-normalized optoacoustic signal (H/E_0) on the fraction of energy absorbed ($1 - 10^{-A}$) for **3** and a calorimetric reference ($CuCl_2$). Effective acoustic transit time, τ'_a = 110 ns; λ^{exc} = 600 nm.

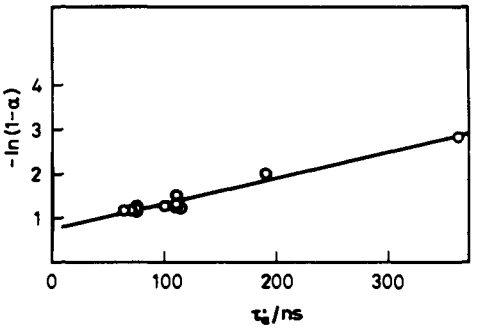

Figure 9. LIOAS: Logarithmic plot of the fraction of heat ($1 - \alpha$) stored after excitation of **3** in methanol ($\leq 2.5 \times 10^{-5}$ M) vs the effective acoustic transit time (τ_a').

(35) (a) Patel, C. K. N.; Tam, A. C. *Rev. Mod. Phys.* **1981**, *53*, 517–550. (b) Lai, H. M.; Young, K. *J. Acoust. Soc. Am.* **1982**, *72*, 2000–2007. (c) Heritier, J. M. *Opt. Commun.* **1983**, *44*, 267–272. (d) Tam, A. C. *Rev. Mod. Phys.* **1986**, *58*, 381–431.

(36) When short excitation pulses (with respect to the acoustic transit time) are used, the amplitude of the first trough of the LIOAS signal relates to the lifetime of the species-storing part of the absorbed light energy.[14c,35b,c] We therefore monitored the amplitude as a function of the heat integration time—as an alternative to complex mathematical data treatment—in order to obtain time-resolved LIOAS results.

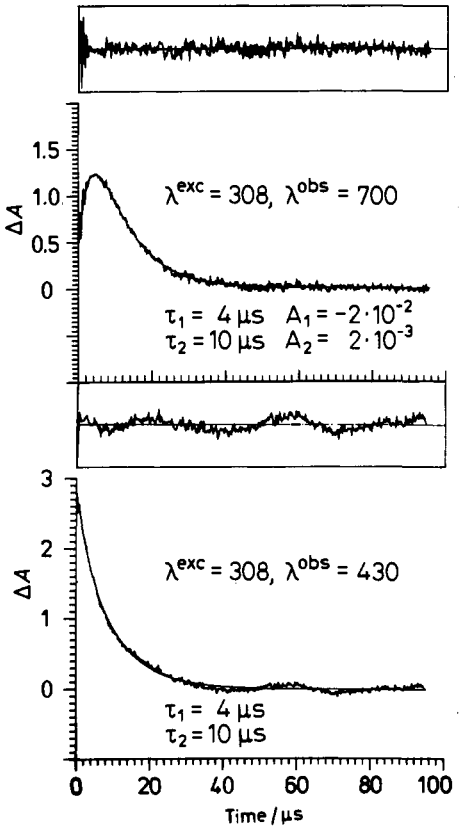

Figure 10. Time-resolved difference absorbance changes (×10) of a 320 μM benzene solution of anthracene excited at 308 nm in the presence of 50 μM **3** and monitored at two different λ^{obsd} values. For each decay curve the distribution of errors for a sum of two single-exponential decays is displayed. The low-frequency noise of the bottom decay is an instrumental artifact.

Logarithmic plots of the fraction of energy $(1 - \alpha)$ stored within the experimental LIOAS time window (i.e., of the energy consumed by processes competing with prompt heat dissipation, such as product formation) as a function of τ_a' were linear as depicted for **3** in Figure 9. The linearity of these plots indicates that the energy-storing product decays in a unimolecular process with a rate constant within the range of variation in $1/\tau_a'$. Since fluorescence can be neglected (Φ_f ca. 10^{-3}; vide supra), the dependence of $(1 - \alpha)$ on τ_a' can be described by eq 1, where ν is the excitation frequency, N_A Avogadro's number, h Planck's constant, ΔE_P^0 the molar energy content (at zero time after excitation) of the energy-storing product of lifetime τ_P, and Φ_P the quantum yield of its formation.[14a,c,35]

$$-\ln (1 - \alpha) = -\ln [\Phi_P \Delta E_P^0 / N_A h\nu] + \tau_a'/\tau_P \qquad (1)$$

The slope in Figure 9 affords the lifetime of the energy-storing product, $\tau_P = 170 \pm 20$ ns, and from the intercept a value of 0.72 $\pm$ 0.08 kJ/mol for $\Phi_P \Delta E_P^0$ is obtained. The respective values of $3H^+$ ($<1.5 \times 10^{-5}$ M; $\lambda^{exc} = 690$ nm) are 160 $\pm$ 30 ns and 0.8 $\pm$ 0.1 kJ/mol.

Triplet Quantum Yield Determination. Analogous to observations with biliverdin dimethyl ester (**4**),[37] direct excitation of **3** in toluene, benzene, and methanol within either the red or blue absorption band did not produce any transient absorption.

By using the flash-photolytic energy transfer method,[16] triplet anthracene, generated in 320 and 160 μM benzene solutions with $\lambda^{exc} = 308$ nm, was quenched by **3** with a quenching rate constant of $k_q = (6 \pm 2) \times 10^9$ M^{-1} s^{-1}. The decay of the absorption of triplet anthracene at 430 nm in the presence of **3** could be fitted to a sum of two single exponential terms with lifetimes of 3–6 μs (depending on [**3**]) and 10 μs (Figure 10 bottom). At 700 nm,

(37) Land, E. J. *Photochem. Photobiol.* **1979**, *29*, 483–487.

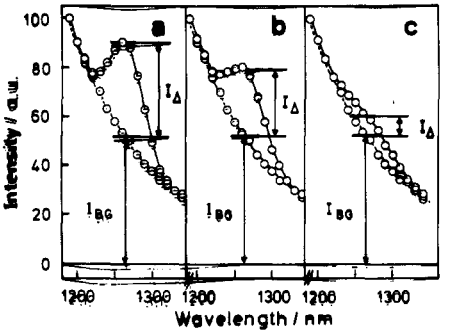

Figure 11. Steady-state near-IR emission of aerated neutral and acidified carbon tetrachloride solutions of **3**; concentrations: (a) 2 μM **3** + 0.2 M trifluoroacetic acid, (b) 10 μM **3** + 0.2 M trifluoroacetic acid, and (c) 10 μM **3**. The $O_2(^1\Delta_g)$ luminescence intensity, I_Δ, and background luminescence intensity, I_{bg}, are marked.

an absorption increase (negative amplitude) with the shorter lifetime (4 μs in the case shown in Figure 10) and a subsequent decay with a 10-μs lifetime were observed (Figure 10 top). This means that the absorption of ^{3}**3** appears at 700 nm with the same time constant (4 μs) as the decay of triplet anthracene at 430 nm. The absorption of ^{3}**3** decayed with a lifetime of 10 μs at both 430 and 700 nm.

The absorption coefficient of ^{3}**3** was obtained from the triplet anthracene quenching by extrapolating the absorbance of the donor triplet anthracene at 430 nm (ΔA_D, Figure 10 bottom) and that of ^{3}**3** at 700 nm (ΔA_A, Figure 10 top) to the end of the laser pulse. Equation 2 was used to calculate the ratio between the molar absorption coefficients for acceptor (ϵ_A) and donor (ϵ_D) at the respective observation wavelengths:[38]

$$\epsilon_A^{700}/\epsilon_D^{430} = (\Delta A_A/\Delta A_D)(k_D + k_q[3] - k_A)/(k_q[3]) \qquad (2)$$

In eq 2, k_D is the rate constant for the decay of the donor triplet anthracene in the absence of **3**, and k_A is the rate constant for the decay of the acceptor triplet (^{3}**3**). From $\epsilon_D^{430} = 4.5 \times 10^4$ M^{-1} cm^{-1},[16] a value of $\epsilon_A^{700} = (3 \pm 0.5) \times 10^4$ M^{-1} cm^{-1} is calculated. From a similar extrapolation of the absorbance of ^{3}**3** at $\lambda_{max} = 400$ nm results a value of $\epsilon_A^{400} = (10 \pm 2) \times 10^4$ M^{-1} cm^{-1}.

With the absorption coefficient of ^{3}**3**, and taking into account that the absorbance at 700 nm of this triplet formed upon direct excitation of a 50 μM solution of **3** (using a 60 mJ pulse, which should be saturating) was $\Delta A_{700} < 10^{-3}$, an upper limit of [^{3}**3**] $< 10^{-8}$ M is obtained, which affords $\Phi_{isc} <$ ca. 2×10^{-4} as a maximum value for the S → T intersystem crossing quantum yield of **3**.

Formation and Quenching of Singlet Molecular Oxygen. Singlet oxygen, $O_2(^1\Delta_g)$, is produced upon sensitization by ^{3}**3** and by ^{3}**3**H$^+$. Its characteristic near-IR phosphorescence centered at 1270 nm was superimposed on broad background fluorescence from the bilatriene (Figure 11). The 1270-nm luminescence in acidified solution was stronger than that in neutral solution (cf. Figure 11b,c). The assignment of this luminescence to $O_2(^1\Delta_g)$ is based on the following findings: (i) The ratio of the intensities of the emission band at 1270 nm and of the background decreased upon increasing [**3**H$^+$] (Figure 11a,b). (ii) The phosphorescence decayed monoexponentially in carbon tetrachloride (19 μM **3**, λ^{exc} = 600 nm), 1,3-dibromobenzene (12 μM, λ^{exc} = 600 nm), and benzene (13 μM, 560 nm) with lifetimes of 210,[39] 39, and 30 μs, respectively, and it was quenched with triethylamine and β-carotene (Figure 12). (iii) Furthermore, **3** and **3**H$^+$ also quenched the emission when generated by other sensitizers. Thus, the emission, when sensitized by 2 μM *meso*-tetraphenylporphine in aerated benzene-d_6, was quenched by **3** (3–30 μM), the absorbance by the porphine at $\lambda^{exc} = 420$ nm being at least ten times that

(38) Carmichael, I.; Hug, G. L. *J. Phys. Chem. Ref. Data* **1986**, *15*, 1–250.
(39) For an $O_2(^1\Delta_g)$ lifetime in carbon tetrachloride with a nonreactive sensitizer, $\tau_\Delta^0 = 26$ ms, see: Salokhiddinov, K. I.; Buteva, I. M.; Dzhagarov, B. M. *Opt. Spectrosc.* **1979**, *47*, 487–490.

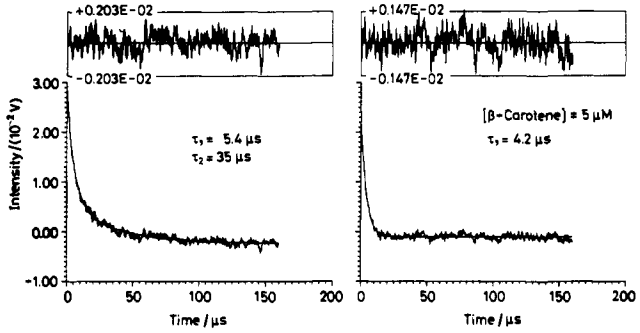

Figure 12. $O_2(^1\Delta_g)$ phosphorescence decay upon laser-pulse excitation at 560 nm of an aerated benzene solution of **3** (13 μM) in the absence (left) and in the presence (right) of β-carotene. The decay in the absence of β-carotene was fitted to a sum of two single-exponential terms, the shorter lifetime being attributed to instrumental factors and the longer lifetime to the $O_2(^1\Delta_g)$ emission. The distributions of fitting error are added on top.

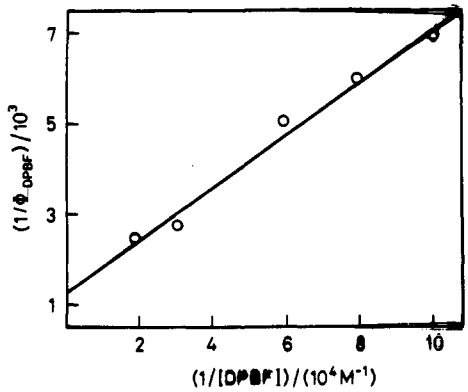

Figure 13. Double reciprocal plot of the quantum yield of diphenylisobenzofuran (DPBF) bleaching vs quencher concentration in aerated toluene solutions of **3** (3.5 μM); λ^{exc} = 597 nm, λ^{obsd} = 415 nm.

of **3**. In view of the bleaching of **3**, the solution was changed after one or two laser pulses for the purpose of signal averaging. A linear Stern–Volmer plot afforded a quenching rate constant of $k_q = (3.4 \pm 0.4) \times 10^8$ M^{-1} s^{-1}. An analogous quenching experiment with $3H^+$ (50–450 μM) and hematoporphyrin (10 μM) as an $O_2(^1\Delta_g)$ sensitizer (λ^{exc} = 532 nm in aerated acidic carbon tetrachloride) gave $k_q = (4.3 \pm 0.3) \times 10^7$ M^{-1} s^{-1}.

Since saturating laser energies are needed to generate the $O_2(^1\Delta_g)$ phosphorescence signal by sensitization with ^{3}**3**, extrapolation of the time-resolved emission intensity to zero time could not be used for the quantum yield determination of $O_2(^1\Delta_g)$ formation, Φ_Δ, by the comparative method. Instead, Φ_Δ was measured by monitoring the bleaching of a chemical quencher of $O_2(^1\Delta_g)$, diphenylisobenzofuran,[19] upon steady-state irradiation of **3**. The actinometrically determined number of absorbed photons and the double reciprocal plot of the bleaching quantum yield vs quencher concentration (Figure 13) gave a value of $\Phi_\Delta = (8 \pm 6) \times 10^{-4}$. The rate constant obtained for the reaction of $O_2(^1\Delta_g)$ with diphenylisobenzofuran was $k_r = (7 \pm 8) \times 10^8$ M^{-1} s^{-1}, in good agreement with the literature value (8×10^8 M^{-1} s^{-1}).[40]

Discussion

Conformational Heterogeneity of 3 in Solution. The appearance of two bands each for fluorescence and fluorescence excitation of **3** in low concentrations in methanol (Figures 1–3) and toluene (spectra not shown) are attributed to two families of conformers of the bilatriene, quite analogous to the previous assignment made for **4**.[2,12] The ratio of the oscillator strengths of UV to visible absorption bands is a measure of bilatriene conformation, a large ratio relating to a helically coiled form and a small ratio reflecting some degree of stretching of the chain.[1,42] Since the areas of the overlapping fluorescence excitation bands are difficult to estimate, the ratio of their intensity (reflecting the absorption coefficient of the excited species) in the near UV to that in the visible wavelength region—rather than the oscillator strengths—normally serves to judge the conformation(s) detected by fluorescence. Thus at low concentrations, values of $\epsilon_{UV}/\epsilon_{VIS} = 1.2$ for the species of **3** emitting at 633 nm (Figure 1c) and 1.6 for the species emitting at 680 nm (Figure 1b) indicate a more stretched conformation for the former, which is further characterized by an excitation band with λ^{exc}_{max} = 340 nm and by narrower and more structured band shapes. The emission band of the helically coiled conformation with the greater $\epsilon_{UV}/\epsilon_{VIS}$ value is broader, and the excitation maxima are at 400 and 580 nm (Figure 3a).

Concentration changes affect the relative population of both families of conformers. When the concentration is increased, the stretched forms decrease and a broadening of the emission in the red flank sets in (Figure 3a). The emission maximum at 705 nm, which appears at even higher concentrations with excitation maxima at 400 and 574 nm, is attributed to dimers and/or to larger aggregates. The separation of emission and excitation spectra of the two families of conformers of **3** proved more difficult than it has been to separate the spectra of the two conformational types of **4** by an appropriate choice of excitation wavelengths.[2,12]

While the emission and excitation spectra allow the characterization of and differentiation between the two principal families of conformers, the relative population of either component can be judged from a comparison of the $\epsilon_{UV}/\epsilon_{VIS}$ value in the absorption spectrum and of the band shape with the corresponding features of the excitation spectra of **3** (Figure 1b,c). As has been the case also with **4**, the helically coiled form of **3** appears to be more abundant in the solvents studied.

Mechanism of Self-Sensitized Photooxidation. Generation of $O_2(^1\Delta_g)$. The presence of $O_2(^1\Delta_g)$, which is observed by steady-state and time-resolved near-IR emission (Figures 11 and 12), in prerequisite for the photobleaching of the bilatriene. Thoroughly degassed solutions in any solvent were not bleached even after prolonged irradiation.[43] In view of the generation of $O_2(^1\Delta_g)$ upon sensitization by the bilatriene and of the solvent and solvent-induced D/H effects on the photoreaction, the photobleaching and formation of products **7–10** can be understood only in terms of a type II photooxidation mechanism,[44] i.e., production of $O_2(^1\Delta_g)$ sensitized by ^{3}**3** and subsequent oxidation of **3** by $O_2(^1\Delta_g)$. Singlet-state quenching need not be considered as an alternative. Similar fluorescence yields for **3** and **4** suggest that the lifetimes of ^{1}**3** and ^{1}**4** should also be similar (viz. 20 ps for the coiled and ca. 1.5 ns for the stretched conformers of **4**[10]) and too short to be quenched by ground-state oxygen. $O_2(^1\Delta_g)$ is therefore exclusively formed by triplet energy transfer from ^{3}**3**.

The formation of the triplet bilatriene, ^{3}**3**, has been established unequivocally, although direct excitation of neither **3** nor $3H^+$ revealed any optically detectable intermediate in flash photolysis. Similar attempts with all other bilatrienes studied so far [e.g., **4**[37] and (3'*S**)-**5**] were equally unsuccessful. However, the triplet state of **3** was detected by flash-photolytic energy transfer experiments, with an estimated intersystem crossing yield of $\Phi_{isc} < 2 \times 10^{-4}$. This low value correlates with the equally low yield for the sensitized formation of $O_2(^1\Delta_g)$, $\Phi_\Delta = (8 \pm 6) \times 10^{-4}$, obtained by chemical quenching of $O_2(^1\Delta_g)$ with 1,3-diphenylisobenzofuran. A quantum yield of bleaching of $\Phi_{bl} = 5 \times 10^{-5}$ was calculated from eq 3, which makes the quenching of $O_2(^1\Delta_g)$ by **3** into account,

(40) A rate constant of $k_r = 8 \times 10^8$ M^{-1} s^{-1} was reported for the reaction of $O_2(^1\Delta_g)$ with diphenylisobenzofuran in methanol.[41]

(41) Merkel, P. B.; Kearns, D. R. *J. Am. Chem. Soc.* **1972**, *94*, 7244–7253.

(42) Burke, M. J.; Pratt, D. C.; Moscowitz, A. *Biochemistry* **1972**, *11*, 4025–4031. Chae, Q.; Song, P.-S. *J. Am. Chem. Soc.* **1975**, *97*, 4176–4179. Wagnière, G.; Blauer, G. *Ibid.* **1976**, *98*, 7806–7810.

(43) Purging of the solutions with argon is not sufficient for suppression of the photobleaching. Since the reaction has to be carried out with [**3**] < 10^{-4} M for solubility reasons, the remaining estimated concentration of [O_2] = 10^{-6} M was sufficient for reaction with the low [^{3}**3**].

(44) Foote, C. S. In *Singlet Oxygen*; Wasserman, H. H., Murray, P. W., Eds.; Academic Press: New York, 1979; pp 139–176.

$$\Phi_{bl} = \Phi_\Delta k_q[3]/(k_q[3] + k_d) \quad (3)$$

with [3] = 20 μM and $k_q = 3.4 \times 10^8$ M^{-1} s^{-1} (in toluene). This value is in reasonable agreement with the steady-state determination of the yield for photochemical conversion, Φ_{-3} ca. 2×10^{-4}, considering the rather large errors in this measurement.

The detection of $O_2(^1\Delta_g)$ in nonhalogenated solvents unequivocally demonstrates its formation by energy transfer from ^{3}**3** (Figure 12) and thus provides the first example of direct $S_1 \rightarrow T_1$ intersystem crossing in a bilatriene. However, since $O_2(^1\Delta_g)$ can also be formed by the reaction of superoxide ion with halocarbons,[45] the mechanism of $O_2(^1\Delta_g)$ generation is debatable when carbon tetrachloride (e.g., see Figure 11) and 1,3-dibromobenzene are used as the solvents (but not when benzene and toluene are used instead!). Should **3** have primarily formed O_2^-, the detected $O_2(^1\Delta_g)$ could have arisen from a secondary reaction.

The dependence of the photobleaching of **3** on excitation wavelength (Figure 7) reflects the conformational heterogeneity of the bilatriene in solution as recognized above from its fluorescence and fluorescence excitation data. The quantum efficiency of bleaching is highest at 577 nm where the helically coiled **3** absorbs predominantly, and it is lowest at 597 nm where stretched conformers absorb most. It follows that the coiled **3** is more efficiently bleached than the more stretched conformers. Accordingly, the $O_2(^1\Delta_g)$ addition and C-5^L–C-5^R bond formation selectively occur with the coiled conformers (see below). Either or both of two reasons may account for this conformational selectivity: (i) The S → T intersystem crossing quantum yield, Φ_{isc}, may be higher for the coiled form, which would also result in a higher Φ_Δ value, and (ii) the coiled conformer may be more reactive toward $O_2(^1\Delta_g)$. Regrettably, the very low upper limit for the S → T intersystem crossing of **3**, Φ_{isc} < ca. 2×10^{-4} precluded a monitoring of Φ_{isc} as a function of λ^{exc}. Further information regarding point (i) is therefore not yet available.

Role of $O_2(^1\Delta_g)$ in Photobleaching of 3. This role is established by the observation of solvent and solvent-induced D/H isotope effects on the reaction, and by the fact that **3** both sensitizes the formation of $O_2(^1\Delta_g)$ and quenches this reactive species. The solvent effects on the rate constant of conversion, k_{-3}, which is smaller in methanol/triethylamine than in toluene, parallel the trend of the $O_2(^1\Delta_g)$ lifetime, which is much shorter in the former solvent than in the latter.[46]

In the calculation of the D/H isotope effects, the quenching of $O_2(^1\Delta_g)$ by **3** had to be taken into account. Thus, eq 4 results from a simple quenching mechanism, assuming that neither Φ_{isc} nor Φ_Δ are influenced by isotope substitution:

$$k^D/k^H = (k_d^D + k_q[3])/(k_d^H + k_q[3]) \quad (4)$$

In this equation, $k_d^D = 1/\tau_\Delta^D$ and $k_d^H = 1/\tau_\Delta^H$ are the rate constants for the decay of $O_2(^1\Delta_g)$ in deuterated and nondeuterated solvent, respectively, and the rate constant for the quenching of $O_2(^1\Delta_g)$ by **3** is $k_q = 3.4 \times 10^8$ M^{-1} s^{-1} (determined in benzene-d_6). With τ_Δ^D = 320 μs and τ_Δ^H = 29 μs in toluene-d_8 and in toluene, respectively,[47] and [3] = 1.5×10^{-5} M, a calculated value of k^D/k^H = 5.04 is obtained, which is even larger than the significant measured value (k^D/k^H = 2). For methanol-d_4 and methanol [with τ_Δ^D = 227 μs[48] and τ_Δ^H = 9.5 μs (Krasnovsky[46]), respectively, and the above k_q value], k^D/k^H = 11 is calculated for [3] = 1.9×10^{-5} M, which is within the error of the experimental k^D/k^H = 9. These considerable isotope effects clearly support a participation of $O_2(^1\Delta_g)$ in the photobleaching process. The difference between the calculated and the experimental ratios k^D/k^H is possibly due to the presence of variable trace amounts of water, an efficient $O_2(^1\Delta_g)$ quencher.

The role of $O_2(^1\Delta_g)$ is further supported by the observation that the photobleaching can also be sensitized with rose bengal, that this sensitization is inhibited by the $O_2(^1\Delta_g)$ quencher diazabicyclooctane and not in the least by the peroxide structure of products **8–10**.

Formation of Oxidation Products 7–10. The structures of both product types, **7** and **8–10**, clearly demand an attack of $O_2(^1\Delta_g)$ on the C-4,5 double bond of **3**. Product structures such as the tricyclic aldehyde **7** and 3-methyl-4-ethylidenesuccinimide (not isolated) are a well-precedented result of dioxetane formation and subsequent thermal cleavage. A dioxetane including C-4 and C-5 could arise directly upon a [2 + 2] addition of $O_2(^1\Delta_g)$. In view of the unsymmetric nature of the double bond with the low electron density of C-5,[5,49] it could also arise from a selective $O_2(^1\Delta_g)$ attack at C-4, resulting in an O_2 adduct that could be a common precursor of **7–10**. Thus, this intermediate could cyclize to the dioxetane and, alternatively, form a bond between its own C-5 position and that of a second ground-state molecule of **3**. The dependences of the ratio **7**/(**8–10**) on [O_2] and of the bleaching rate constant, k_{-3}, on [**3**] in oxygen-poor solution are in accord with this mechanism.[50] We should point out, however, that this work does not provide any further mechanistic clues, in particular none concerning the details of the steps leading to **8–10**.

Photoisomerization. The LIOAS study revealed that irradiation of **3** in degassed and oxygen-containing solutions leads to an intermediate with a lifetime of ca. 170 ns. Products of *E*,*Z* photoisomerization around the C-3,3′, C-4, and C-15 double bonds can be ruled out. The 3,3′-*Z* isomer **12**[29] is excluded since the LIOAS results with **5**, which lacks the C-3 ethylidene double bond, were quite similar to those with **3**. Furthermore, the 4-*E* and 15-*E* isomers of **3** are known to be thermally stable compounds.[51] *Z* → *E* isomerization around the C-10 bond to form the 10-*E* isomer of **3** therefore remains the most probable candidate to represent the 170-ns intermediate. The failure to observe any transient absorbance in the flash photolysis of **3** indicates that the 10-*E* isomer and its parent compound possess very similar absorption coefficients.

The excitation wavelengths leading to the largest energy storage (i.e., the smallest α values; see Table III) coincide with the absorption maximum of the stretched conformers (λ_{max}^{exc} = 623 nm; cf. Figures 1–3). In the flanks of the absorption band, where the coiled form absorbs predominantly, α is larger and even equals unity when measured for the same acoustic transit time as for the other wavelengths. The 10-*E* intermediate thus is preferentially formed from stretched forms of **3**, a conformational selectivity that had already been suggested also for **4** by results obtained by irradiation of liquid low-temperature solutions and monitoring by difference absorption spectroscopy[52] and by a LIOAS study at room temperature with a ceramic piezoelectric detector.[6] It is also interesting to note that the biliverdin IXγ and IXδ dimethyl esters show a similar selectivity in their photochemical reactivity; only the stretched conformers afford the products of ring closure between the central pyrrole rings, phorcabilin and neobiliverdin IXδ, respectively.[9] The fact that the α values tend to unity at

(45) Kanofsky, J. R.; Sugimoto, H.; Sawyer, D. I. *J. Am. Chem. Soc.* **1988**, *110*, 3698–3699.

(46) The lifetimes of $O_2(^1\Delta_g)$ are τ_Δ = 9.5 μs in methanol (Krasnovsky, A. A., Jr. *Chem. Phys. Lett.* **1981**, *81*, 443–445) and 29 μs in toluene (D. Mârtire, Unpublished results; Salokhiddinov et al.[39]). The addition of triethylamine to the methanol solution shortened τ_Δ below the threshold of time resolution of our $O_2(^1\Delta_g)$ detection system.

(47) Salokhiddinov, K. I.; Byteva, I. M. *Opt. Spectrosc.* **1983**, *55*, 282–284.

(48) Rodgers, M. A. J. *J. Am. Chem. Phys.* **1983**, *105*, 6201–6205.

(49) Yamaguchi, K. In *Singlet Oxygen*; Frimer, A. A., Ed.; CRC Press: Boca Raton, FL, 1985; Vol. 3, pp 119–251.

(50) Scheer and Krauss[4,30b] have previously proposed a dimeric structure joined across a C-5^L–C-5^R bond for one of the major products (a cyclobutane derivative involving carbons 4 and 5 of both halves) of the anaerobic photooxidation of octaethyl A-dihydrobilindione with iodine.

(51) Thümmler, F.; Rüdiger, W. *Tetrahedron* **1983**, *39*, 1943–1951. Thümmler, F.; Rüdiger, W.; Cmiel, E.; Schneider, S. *Z. Naturforsch.* **1983**, *38c*, 359–368. Rüdiger, W. *Phil. Trans. R. Soc. London* **1983**, *B303*, 377–386. Falk, H.; Grubmayr, K.; Kapl, G.; Müller, N.; Zrunek, U. *Monatsh. Chem.* **1983**, *114*, 753–771. Rüdiger, W.; Thümmler, F.; Cmiel, F.; Schneider, S. *Proc. Natl. Acad. Sci. B* **1983**, *80*, 6244–6248.

(52) Braslavsky, S. E.; Holzwarth, A. R.; Langer, E.; Lehner, H.; Matthews, J. I.; Schaffner, K. *Isr. J. Chem.* **1980**, *20*, 196–202. See also: Braslavsky, S. E.; Holzwarth, A. R.; Langer, E.; Lehner, H.; Matthews, J. I.; Schaffner, K. *Photoreceptors and Plant Development, Proc. Eur. Plant Photomorphogenesis*; de Greef, J. A., Ed.; University Press: Antwerp, 1980; pp 89–100.

higher concentrations of **3** (Figure 8) indicates that aggregates photoisomerize less readily.

A lower limit of $\Phi_p \leq 0.5 \pm 0.04$ for the quantum yield of formation of the 10-*E* isomer ($\lambda^{exc} = 600$ nm) can be estimated from eq 1, the intercept of 0.72 ± 0.08 kJ/mol in Figure 9, and $\nu = 628$ nm for the 0–0 band of **3** (Figures 1 and 2). This calculation is based on the assumption that product formation from the excited state of **3** is exothermic, and it accounts neither for the negligible yields of fluorescence ($\Phi_f \approx 10^{-3}$) and triplet formation ($\Phi_{isc} < 10^{-3}$)—the latter being another energy-storing process—nor for the $E \rightarrow Z$ isomerization around the C-3,3′ double bond, which should not be essential in view of the fact that compounds lacking this double bond gave similar results. The calculation also neglects a possible photochemical back-isomerization.[53] Should a photochromic equilibrium be established within the duration of the laser pulse, the rate of thermal deactivation of the transient photoisomer would in fact be slower (thus prolonging the measured lifetime, $\tau_P = 170 \pm 20$ ns, which is rather short for a ground-state intermediate) and the quantum yield of its formation would be smaller. In any case, the optoacoustic data indicate that photoisomerization is a substantial radiationless deactivation process of excited **3**.

Conclusions

The absorption, steady-state fluorescence, and fluorescence excitation results with phycocyanobilin dimethyl ester (**3**) and the 3,3′-dihydro-3′-thioethoxy derivative **5** in the solvents studied are very much like those obtained previously with biliverdin dimethyl ester (**4**).[2] Both fluoresce only weakly ($\Phi_f \sim 10^{-3}$) and, in the ground state, populate two families of conformers, the more abundant being helically coiled and the other being more stretched.

The $S \rightarrow T$ intersystem crossing, with a value of $\Phi_{isc} < 10^{-4}$ estimated from energy-transfer experiments with **3**, correlates with a quantum yield of $\Phi_\Delta = (8 \pm 6) \times 10^{-4}$ for the formation of $O_2(^1\Delta_g)$ upon sensitization with ^{3}**3**. This production of $O_2(^1\Delta_g)$ represents for the first time evidence for the population by $S \rightarrow T$ intersystem crossing of the triplet state in a bilatriene.

Photoisomerization of **3** and **5**, most probably by $Z \rightarrow E$ rotation around the C-10 double bond, preferentially occurs with the stretched conformers and affords transients that thermally revert back to the starting material in ≥200 ns at room temperature. The reaction appears to be a major deactivation process of excited bilatrienes, together with rapid proton exchange between the central nitrogens,[2] as established for **4**[10] and for model *Z*,-syn-periplanar dipyrrole compounds.[54] In the case of **3**, isomerization around the C-3 ethylidene double bond[29] is an additional, albeit less efficient, deactivation channel.

The self-sensitized type II photooxidation of **3** (with a value of $\Phi_{-3} = 2 \times 10^{-4}$ compatible with the similarly low Φ_Δ) to products **7–10** preferentially occurs with the helically coiled conformers. An analogous reactivity is also exhibited by the 3,3′-dihydro-3′-methoxy derivate **6**, whereas the protonated form of phycocyanobilin dimethyl ester, **3H**$^+$, is not photooxidized although it sensitizes oxygen to $O_2(^1\Delta_g)$ considerably more efficiently.

It is conceivable that photoproducts of type **7–10** are also formed in biological media when exposed to $O_2(^1\Delta_g)$, e.g., in the photodynamic therapy of tumors[11] or in light-harvesting biliproteins such as phycocyanin. We have followed up a speculation that the photophobic response of certain microorganisms, e.g., the alga *Anabaena variabilis*,[55] might be regulated by phycocyanin-sensitized generation of $O_2(^1\Delta_g)$, which could damage the surrounding biliprotein as long as the organism is prevented from avoiding the light field. However, attempts to detect in vivo $O_2(^1\Delta_g)$ phosphorescence from *A. variabilis* were not successful. This failure is possibly due to the relatively low sensitivity of our instrumentation in recording $O_2(^1\Delta_g)$ in H_2O and D_2O, considering the small values for its τ_Δ in H_2O[41,48] and for its radiative rate constants in H_2O and D_2O.[56] In addition, the lifetime of $O_2(^1\Delta_g)$ might be further shortened by its high reactivity in such a situation, as has been discussed for living tissues.[57]

Acknowledgment. We thank J. Bitter, B. Dittrich, U. Harms, K. Herbrand, A. Keil, G. Koç-Weier, D. Lenk, M. Massau, W. Schmöller, B. Slykers, and G. Wojciechowski for able technical assistance. We are also indebted to Dr. J. Grotemeyer and Professor E. W. Schlag (Universität München) for the REMPI-RETOF mass spectra, to Dr. M. Linscheid (Universität Dortmund) for the FAB mass spectra, and to Dr. J. Awruch (Universidad de Buenos Aires, recipient of a fellowship from the Deutschen Akademischen Austauschdienst, D.A.A.D.) for valuable discussions. Professor W. Nultsch (Universität Marburg) provided the alga *Anabaena variabilis* and offered helpful advice. K.H. and S.N. were supported by fellowships from the Alfried Krupp von Bohlen und Halbach-Stiftung and the D.A.A.D., respectively.

(53) Kinetic and thermodynamic parameters can be extracted from the LIOAS data of photochromic systems where the thermally labile photoisomers are detected optically and have lifetimes in the nano- to millisecond range; see, for examples, the investigations of phytochrome,[14b] of polymethine laser dyes (Bilmes, G. M.; Tocho, J. O.; Braslavsky, S. E. *J. Phys. Chem.* **1988**, *92*, 5958–5962; *Ibid.* **1989**, *93*, 6696–6699), and of bacteriorhodopsin (Rohr, M.; Gärtner, W.; Braslavsky, S. E. Unpublished results).

(54) Falk, H.; Grubmayr, K.; Neufingerl, F. *Monatsh. Chem.* **1979**, *110*, 1127–1146.

(55) Schuchart, H.; Nultsch, W. *J. Photochem.* **1984**, *25*, 317–325.

(56) Nonell, S. Ph.D. Thesis, Institut Químic de Sarrià, Barcelona, Spain, and MPI für Strahlenchemie, Mülheim a. d. Ruhr, Germany, 1988. Schmidt, R.; Brauer, H.-D. *J. Phys. Chem.* **1990**, *94*, 4377–4378. Scurlock, R. D.; Ogilby, P. R. *J. Phys. Chem.* **1987**, *91*, 4599–4602.

(57) Patterson, M. S.; Madsen, S. J.; Wilson, B. C. *J. Photochem. Photobiol. B: Biology* **1990**, *5*, 69–84.